iScience

CellPress
OPEN ACCESS

Review

Large-scale multimodal surface neural interfaces for primates

Tiphaine Belloir,[1,2] Sergio Montalgo-Vargo,[3] Zabir Ahmed,[3] Devon J. Griggs,[2,4] Shawn Fisher,[1,2] Timothy Brown,[5] Maysamreza Chamanzar,[3,6,7] and Azadeh Yazdan-Shahmorad[1,2,4,*]

SUMMARY

Deciphering the function of neural circuits can help with the understanding of brain function and treating neurological disorders. Progress toward this goal relies on the development of chronically stable neural interfaces capable of recording and modulating neural circuits with high spatial and temporal precision across large areas of the brain. Advanced innovations in designing high-density neural interfaces for small animal models have enabled breakthrough discoveries in neuroscience research. Developing similar neurotechnology for larger animal models such as nonhuman primates (NHPs) is critical to gain significant insights for translation to humans, yet still it remains elusive due to the challenges in design, fabrication, and system-level integration of such devices. This review focuses on implantable surface neural interfaces with electrical and optical functionalities with emphasis on the required technological features to realize scalable multimodal and chronically stable implants to address the unique challenges associated with nonhuman primate studies.

INTRODUCTION

Understanding the neural basis of complex functions and behavior in living animals and humans is a challenging goal that drives a broad multidisciplinary research community. Meeting this goal will not only contribute to our fundamental knowledge of neuroscience mechanisms but it will also help develop effective treatments for neurological disorders. Neural engineering strives to develop advanced technologies with multimodal capabilities such as bidirectional interfaces to record and manipulate neural circuits with high spatial and temporal precision across large areas of the brain. Traditional cortical neural interfaces rely on the electrical mechanisms of neural signaling to interact with the nervous system. Depending on the application, neural interfaces with electrical modalities are generally classified into three categories: penetrating electrodes (most invasive), electrocorticographic (ECoG) electrodes (less invasive) that are placed on the surface of the brain, and electroencephalographic (EEG) electrodes (non-invasive) that can be placed over the scalp (Figure 1). Penetrating neural interfaces are surgically inserted into the brain tissue as close as possible to the cell body (or soma) of targeted neurons and provide the most information-rich brain signals. However, these probes are highly invasive and their implantation is usually limited to recording from the vicinity of the electrodes. Some recent examples are the Neuropixels 2.0 rigid probe[1] flexible penetrating electrodes based on mesh electronics[2] or cylindrically shaped polymer neural probes.[3] EEG neural interfaces are non-invasive because they do not require any surgical procedure and are placed directly on the scalp. The information obtained from EEG is quite limited because it measures the aggregate signal arriving from many neurons and the neural signal is attenuated through the overlying tissues (i.e. dura, bone, and scalp) between the brain and the electrodes. Despite this limitation, EEG signals have already been used successfully in the field of brain to computer interfaces.[4] ECoG neural interfaces are placed on the surface of the brain, either over the dura (epidural) or under the dura (subdural). They require a surgical procedure but are less invasive to the brain tissue than penetrating probes. The brain signal recorded by these surface interfaces is known as electrocorticography and contains more information than EEG interfaces. Within the current state-of-the-art surface interfaces, micro-electrocorticographic arrays (μ-ECoG) with electrode sizes on the order of 150–1000 μm^2 have been used to record local field potentials, multi-unit potentials, and single-unit spikes.[5,6] Among the three types of devices, micro-electrocorticographic (μ-ECoG) arrays, a type of ECoG array with microscale electrode size, provide an appealing compromise between information acquisition, spatial resolution, and invasiveness.[5] Optical techniques are also powerful tools to image and manipulate neural populations. For example, calcium imaging can reveal

[1]Department of Bioengineering, University of Washington, Seattle, WA, USA

[2]Washington National Primate Research Center, Seattle, WA, USA

[3]Department of Electrical and Computer Engineering, Carnegie Mellon University, Pittsburgh, PA, USA

[4]Department of Electrical and Computer Engineering, University of Washington, Seattle, WA, USA

[5]Department of Bioethics & Humanities, University of Washington, Seattle, WA, USA

[6]Department of Biomedical Engineering, Carnegie Mellon University, Pittsburgh, PA, USA

[7]Carnegie Mellon Neuroscience Institute, Pittsburgh, PA, USA

*Correspondence: azadehy@uw.edu

https://doi.org/10.1016/j.isci.2022.105866

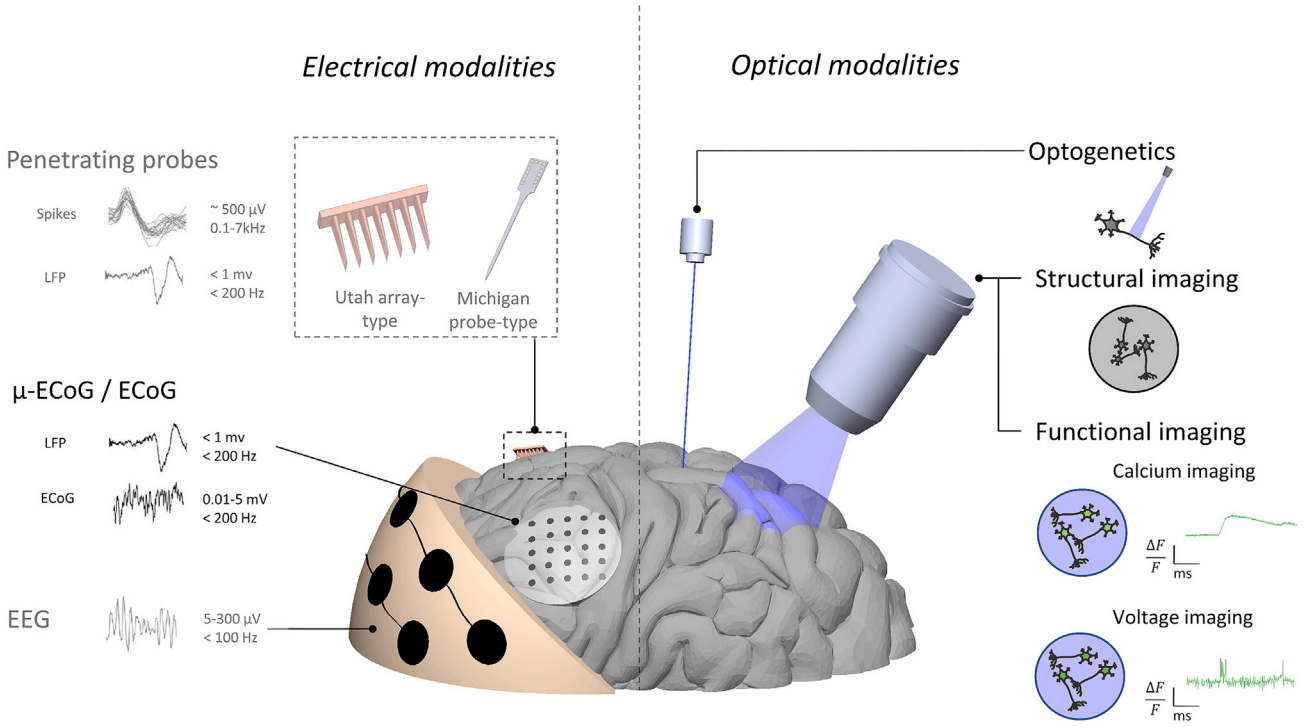

Figure 1. Overview of neural interfaces with electrical and optical modalities

The type of signal recorded is associated with each readout method. For interfaces with electrical modalities, the review focuses on ECoG/µ-ECoG interfaces.

the mechanisms of neural activity at a subcellular scale[7] and optogenetics enables cell-type-specific excitation or inhibition of neurons with millisecond temporal precision,[8] which overcomes the limitations of traditional electrical stimulation. Combining electrical and optical modalities in a single platform could lead to complementary and powerful new ways to explore brain mechanisms and functionality.

Advanced hybrid neural interface technologies with electrical and optical functionalities have already been developed and implemented in small animal models such as rodents. These technologies include penetrating opto-electric neural probes,[9,10] as well as surface transparent electrodes with optical modalities.[11,12] More detailed reviews about these advanced multimodal platforms for rodents can be found elsewhere.[13–15] Translating these advances to clinical testing often requires preclinical studies in large animal models that are closer to humans. Nonhuman primates in particular have evolutionary very similar behavior and cognitive functions to humans, thus making them an important model of study. Novel architecture design concepts, new material platforms and a complete system design and optimization is needed to improve existing interfaces' performance in terms of scalability, multifunctionality, and stability[16,17] and enable their widespread adoption for neuroscience applications in nonhuman primates (NHPs).

In this work, we review ongoing exploratory efforts devoted to address scalability, multimodality, and chronic stability challenges in large animal cortical interfaces with electrical and optical modalities. The first section focuses on large-scale surface interfaces with electrical recording and stimulation capabilities. We will put an emphasis on µ-ECoG technologies. As mentioned previously, µ-ECoG arrays are made of microscale electrodes with contact site diameters many orders of magnitude smaller than traditional ECoG electrode sites and minimized inter-electrode spacing, allowing greater spatial resolution of the measured signals. Most µ-ECoG devices also have ultrathin structure, thereby offering less invasive implantations than traditional ECoG or penetrating electrodes, with minimal tissue response and limited foreign body reaction. In addition, advances in CMOS (Complementary Metal-Oxide-Semiconductor) fabrication techniques now enable an increased number of simultaneous stimulation/recording sites. While this is usually the engineering goal and definition of large-scale cortical interfaces,[17] from a neuroscientific point of view, scalability also implies enlarging the studied area to multiple brain regions by increasing the surface or volume

probed by the recording device. μ-ECoG arrays have the potential for both large coverage and high-density interrogation of neural networks with high temporal resolution. Technological advances in flexible and transparent materials make μ-ECoG arrays appealing candidates to be combined with complementary optical techniques, therefore providing unprecedented methods to study large brain circuits.[18–20] The second section of the review focuses on these large-scale multimodal interfaces combining optical methods and μ-ECoG technologies. In particular, challenges of conducting chronically stable optogenetics experiments in large animal models will be discussed, as well as the combination of this powerful stimulation technique with other optical imaging techniques. Finally, we will discuss challenges and ethical considerations of conducting such advanced neuroscience experiments in large animal models.

Interfaces with electrical modalities

Among the different types of electrophysiological monitoring devices, ECoG arrays are a popular choice in neuroscience due to the optimal compromise between invasiveness and resolution. Additionally, ECoG arrays can be fabricated in various sizes, which can be scaled up to cover large areas of the brain. Recently, advances in electrode fabrication have led the evolution from ECoG to μ-ECoG. Traditional ECoG devices are characterized by spanning large areas of the brain, having low channel count with large electrodes separated by mm scale distances. The clinically available ECoG arrays have electrodes with diameters greater than 1 mm.[5] μ-ECoG devices; on the other hand, they have orders of magnitude smaller electrodes (10 to hundreds of μm) that can be densely packed together. The coverage area is usually smaller in μ-ECoG arrays in comparison to ECoGs. Compared to EEG devices that are placed over the scalp, ECoG arrays are placed beneath the skull via craniotomy. ECoGs can be either placed directly on the surface of the brain (subdural) by removing the native dura, or placed directly on top of the native dura (epidural). The direct contact of ECoG arrays with the surface of the brain can lead to tissue damage and a foreign body response, compromising the quality of the signal recording. To address this issue, soft substrates, such as elastomers, can minimize brain damage and enable chronic long-term application of the ECoG arrays. Having direct exposure to the surface of the brain, however, provides higher temporal and spatial resolution and the ability to record additional types of neural signals. Similar to EEGs, broadband signals at the low frequency range (0–400 Hz), known as local field potentials (LFPs), can be recorded, albeit with higher signal strength compared to EEGs. More importantly, because of the close proximity of ECoG electrodes to the brain, the signal-to-noise ratio is higher and higher frequency signals can also be detected. For ECoG recordings, the amplitudes of the spectral frequency components of the neural signals follow the power law (of LFP), which states that the amplitude of the signal decays by a $1/f^a$ factor, where f is the frequency of the signal and a is a fitting parameter.[21] Despite the lower amplitude content in higher frequencies, high gamma signals can be recorded by μ-ECoG arrays and even spikes have been reported with an electrode size of ~10 μm (neurogrid).[6] In order to record spikes and LFPs, the size of the electrode must be optimized. Ideally, an electrode would be as small as the cell body of a neuron (<10 μm) to achieve single cell detection, but the high impedance associated with such a small electrode will limit the signal-to-noise ratio of the recording. Hence, the size of the electrode must be optimized to achieve a high enough signal-to-noise ratio, while at the same time maintain a high spatial resolution. Additionally, one might think that a higher spatial density in a μ-ECoG would yield to more detailed information about the underlying neural activity. This is not necessarily the case as nearby electrodes in a very dense array might record from the same cluster of neurons. The optimal density of electrodes in a μ-ECoG electrode array interface is not yet investigated systematically. In NHPs, μ-ECoG electrode arrays have been designed with electrode pitch sizes of 250 μm to thousands of μm. Finally, as mentioned earlier, in many practical cases, it is highly desired that the μ-ECoG electrode array be transparent such that the brain tissue can be imaged through the array using optical methods. This enables monitoring of tissue health, global functional imaging of neural activity, and compatibility with optogenetic techniques for neural modulation. In summary, to achieve the desired features of a transparent high-density, large-coverage chronic surface neural interface, the design parameters such as the substrate material, the number, size, density, and material of electrodes, transparency of the array and area of coverage must be optimized. In this section, we review the state of the art in surface electrode array device design, highlighting recent innovations in enhancing functionality and improving scalability. We discuss the challenges of scaling up the size and the number of electrodes to cover large regions of the brain in large animal models and the requirements for translation to humans.

Toward large-scale high-density recording

It is highly desired to design surface neural interfaces with high number of channels in a high-density arrangement. The specific design of the recording electrodes (size, placement, and coverage) depends

on the application. The number of electrodes in an array is usually chosen to be a power of 2 (16, 32, 64, 128, etc.) to be compatible with the back-end electronics. In devices with lower channel count, the signals recorded from individual electrodes can be routed from the detection site to the back-end electronics through dedicated interconnect traces. However, using individual interconnect wires for every electrode represents a great challenge in scalability and in many cases, it is the bottleneck for increasing the density of electrodes. Only a few selections of advanced devices with higher complexity have been demonstrated to work in NHPs with thousands of electrodes,[22,23] (Figure 2). In their work, Chiang et al.[22] developed an actively multiplexed array of NMOS transistors, the "Neural Matrix", for readout across 1008 channels (28 columns, 36 rows) (Figures 2A–2C). Kaiju et al.[23] obtained an array of 1152 electrodes by integrating nine 128-channel arrays together (Figures 2D–2F). A third study used microscale transfer printing techniques to assemble tens of thousands (>32000) of active components (Si-nanomembrane (Si-NM) transistors and inorganic light-emitting diodes) across polymer substrates with areas that could cover a full human brain (150 cm^2).[24] While this approach shows the high potential of wafer-level fabrication for scalability and high channel count, it has not been demonstrated *in vivo* yet. A wide range of electrode sizes ranging from tens of microns to a few hundreds of microns with applications in NHPs have been demonstrated in literature and are summarized in (Table 1). Overall, larger electrodes are commonly used to record high fidelity signals in the lower frequency range. Smaller electrodes (<100 μm^2), on the other hand, can potentially enable recording of single unit activity from the surface of the brain, while at the same time, enabling high-density electrode arrangements with small inter-electrode spacings.[6,25]

Another parameter of interest is the density of electrodes. While recent studies by Yazdan-Shahmorad et al.[28] and others[34] have measured distinct signals using a ~400 μm pitch for the recording sites, the optimum pitch to minimize redundancy while maximizing neural recording information is not yet determined. Over the last decade, there has been significant development in increasing the number of channels and channel density and the electrode coverage area of μ-ECoG arrays. Importance of high-density electrodes for electrocorticographic recording has been studied and validated both theoretically and experimentally. In particular, higher frequency components of neural signals in human brain have been shown to demonstrate spatial variation in sub-millimeter scale which necessitates the use of dense μ-ECoG arrays.[35] Moreover, it has been shown that densely distributed small electrodes can enable detection of abnormal high-frequency oscillations, which is a potential indicator of epileptic seizure foci.[36,37] Use of higher density arrays in macaque brain has also revealed significant improvement in spatial resolution and signal amplitude. A recent study highlighted the advantages of higher density arrays, showing that a 1152-channel array could more finely map the somatosensory areas in the digit representation of macaque monkeys compared to a standard 128-channel array[23] (Figures 2D and 2E). While the recent advancements in microfabrication based on high-resolution lithography can be leveraged to implement densely packed microelectrode arrays, there are some challenges to achieve large cortical coverage, while retaining high channel density. The inevitably large channel count of the device poses some difficulty in packaging, interfering with the recording circuitry and online analysis of data. As a result, simultaneous acquisition of data requires multiple connectors and amplifiers or highly customized application-specific components. To simplify the connection of passive μ-ECoG arrays to connectors and recording amplifiers, multiple smaller sub-arrays are often overlaid to achieve high channel count and large sampling area[23,32] (Figure 2F). Another approach to circumvent the challenge of interfacing large numbers of wires from high-channel count μ-ECoG is through multiplexing. On-device multiplexers and amplifier circuits enable transmission of neural signals from a large number of electrodes with a small number of wires. Such devices with high-density active electrode arrays have been implemented by using thin-film transistor technology on flexible substrates and validated in rodents,[38] or with flexible silicon transistor technology and validated in monkeys[22] (Figure 2A).

Electrode and substrate material: Toward stability and multifunctionality

A large variety of materials can be employed to implement recording electrodes in μ-ECoG arrays. The choice of electrode material is usually dictated by the intended application. Particular electrode materials might be preferred based on the frequency bandwidth of interest, the timescale of the experiment (acute versus chronic), the need for electrical stimulation, or optical access for optical stimulation or imaging.

Platinum (Pt) and Gold (Au) are widely used in intracortical and surface electrode arrays because of their stability and biocompatibility in neural tissue. However, Pt or Au electrodes with small surface area have large electrochemical impedances that lower the signal-to-noise ratio of recording and have limited

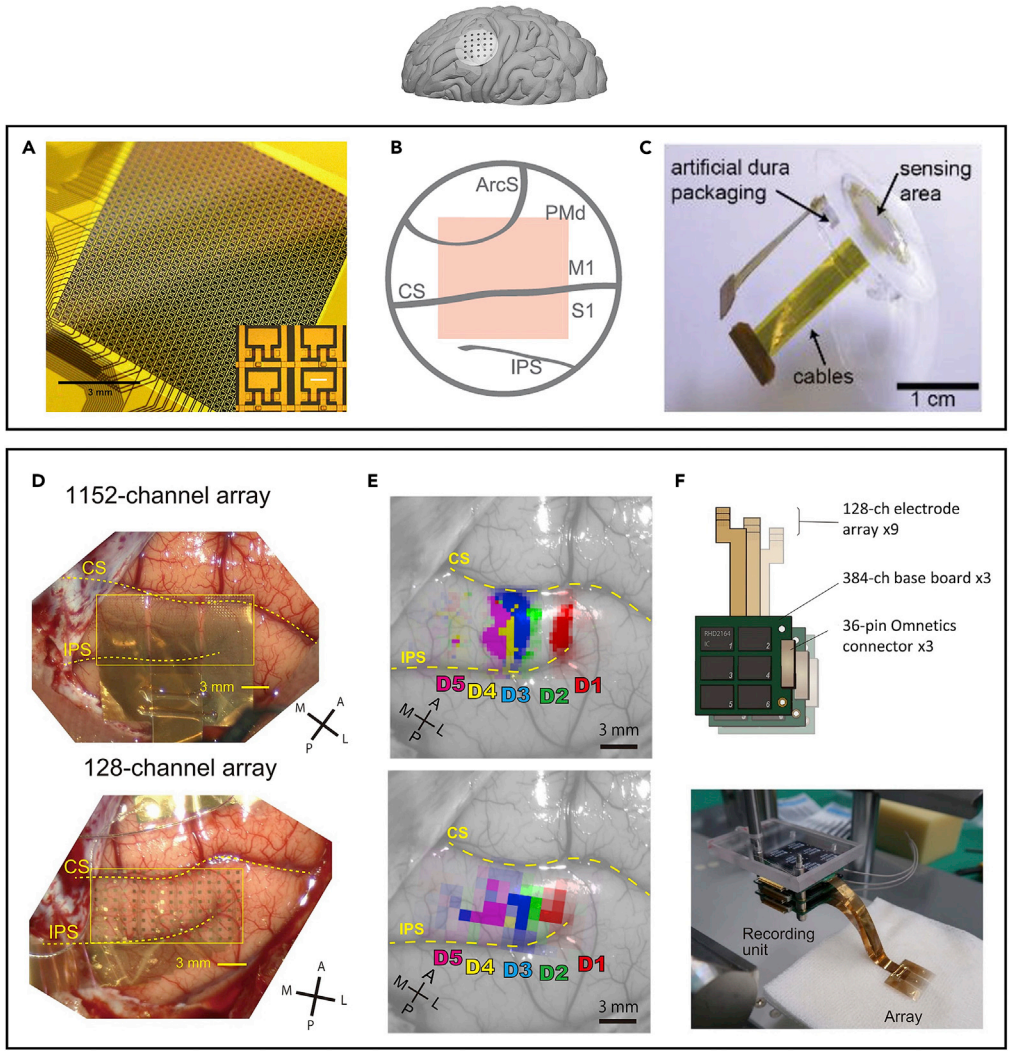

Figure 2. Nonhuman primate μ-ECoG arrays: large scale, high density, high channel count systems

(A) The Neural Matrix: a 1008-ch multiplexed array. Inset: Each electrode is connected to a unit cell consisting of two flexible silicon transistors. Scale bar: 100 μm.

(B) Schematic representation of the electrode array placement on the cortical surface. The circle represents the full implant area; the shaded orange area denotes the region of electrode contacts. The recording area spans premotor, primary motor, and primary sensory cortices. ArcS, arcuate sulcus; CS, central sulcus; IPS, intraparietal sulcus; PMd, dorsal premotor cortex; M1, primary motor cortex; S1, primary sensory cortex.

(C) The neural matrix array and its interconnect cables packaged in an artificial dura for subdural implantation.

(D) Intraoperative views of 1152- (top) and 128- (bottom) channel arrays placed on the cortical surface. For both arrays, the yellow squares indicate the approximate measurement areas. (CS); central sulcus, IPS; intraparietal sulcus.

(E) Somatotopic mapping of digit representation area based on high gamma activity measurements of the somatosensory evoked potentials (SEP) with the 1152-ch array (up) and 128-ch array (down). D1 (red): thumb digit, D2 (green): index digit, D3 (blue): middle digit, D4 (yellow): ring digit, D5 (magenta): little digit.

(F) Configuration diagram (top) and photograph (bottom) showing the stacking strategy used to obtain the 1152-ch array by stacking nine 128-ch arrays and their recording units. *Panels reproduced with permission from:* (A–C,[22] D–F[23]).

current injection capacity for electrical stimulation. Different coating materials are utilized to modify the electrode surface to reduce the impedance while keeping the geometric surface small. Electrodeposition of conductive polymers such as PEDOT:PSS or PEDOT:CNT is shown to improve the charge transfer capacity and reduce the electrochemical impedance in μ-ECoG arrays in rodents.[39,40] In recent years, wafer-scale high-throughput processes of such surface modifications have been developed for integrating PEDOT:PSS,[41] MXene,[42] porous Pt,[43] and glassy carbon.[44,45]

Table 1. NHPs μ-ECoG array features

Study	Year	# channels	Electrode size (×10^3 μm^2)	Spacing (μm)	Density (electrode/mm^2)	Substrate material & total thickness array	Electrode material	Total coverage (mm^2)	Region covered	Additional modalities
Rubehn et al.,[26]	2009	252	785.4 (1000 μm ø)	2000–3000	0.12	Polyimide 14 μm	Pt	2100	motor, sensory and visual cortices	Electrical stimulation
Thongpang et al.,[27]	2011	32	70.69 (300 μm ø)	1000	0.88	Polyimide 24 μm	Cr/Au/Pt	36	Somatosensory and motor cortices	–
Yazdan-Shahmorad et al.,[28]	2016	192 (2 × 96)	5.03 (80 μm ø)	600	1	Parylene C 12 μm	Pt/Au/Pt	192	Somatosensory and motor cortices	Optogenetic modulation
Kaiju et al.,[29]	2017	96	122.5 (350 × 350)	700	2.04	Parylene C 20 μm	Au	47	Somatosensory cortex	–
Komatsu et al.,[30]	2017	64	282.74 (600 μm ø)	1400	0.032	Polyimide/Cu 56 μm	Cu/Ni/Au	~2000	Frontal, parietal, occipital and temporal cortices	Optogenetic modulation
Miyakawa et al.,[31]	2018	60	10 (100 × 100)	1200	0.41	Parylene C 20 μm	Au	144	Inferior temporal cortex (ITC)	Penetrating electrodes
Chiang et al.,[32]	2020	294 (3 × 98)	41.19 (229 μm ø)	610	2.6	Polyimide 31 μm + PDMS molding (100 μm)	Cr/Au	114.4	Prefrontal cortex	–
Chiang et al.,[22]	2020	1008	18 (100 × 180)	250–330	12.12	Polyimide/SiO_2/PDMS 45.5 μm	Si transistors (MOSFETs) + t-SiO2	83.16	Premotor, primary motor and somatosensory cortices	–
Griggs et al.,[33]	2021	32	196.35 500 μm ø	2000	0.25	"Medical grade polymer"	Pt	126	Somatosensory and motor cortices	Electrical stimulation/ imaging (OCTA)
Kaiju et al.,[23]	2021	128	90 (300 × 300)	1000	1	Parylene C 20 μm	Au	128	Somatosensory cortex	–
		1152 (9 × 128)	2.5 (50 × 50)	295	11.75	Parylene C 20 μm	Au + Pt black	98	Somatosensory cortex	–

For applications requiring optical access for stimulation or imaging, Pt and Au are not suitable due to their opacity in the wavelength range of interest. To allow optical access through the μ-ECoG array, Pt and Au wires need to be narrow and sparsely distributed. Yazdan-Shahmorad et al. have demonstrated optogenetic stimulation through μ-ECoG arrays simultaneously with electrical recording.[28] This was enabled by routing the opaque Pt-Au-Pt traces and distributing electrodes in a special way to facilitate optical access through more than 90% of the device area. To achieve even higher channel density while maintaining transparency through the electrodes, different optically transparent and electrically conductive materials can be used as the electrode material. Ultraflexible μ-ECoG devices based on indium tin oxide (ITO) electrodes have been reported for optogenetic stimulation in rodents.[46–48] However, given the lower conductivity of ITO and its brittleness, it has only been used for realizing transparent electrodes but the traces are made of conductive metals.[46] Kwon et al. have demonstrated *in vivo* optogenetic experiments in rodents using transparent μ-ECoG arrays with ITO electrodes and integrated μ-LEDs.[49] Graphene is also utilized as a transparent electrode material to realize μ-ECoG arrays.[50] Park et al. have reported graphene-based μ-ECoG devices for simultaneous electrical recording, optogenetic stimulation, fluorescence microscopy, and 3D coherence tomography in rodents.[11]

Apart from its use as a transparent conductive electrode material for passive μ-ECoG array, graphene is also used for implementing field-effect-based active sensor arrays. In rats, graphene solution-gated field effect transistors (g-SGFETs) have been demonstrated to record infra-slow brain activity with high resolution which is not feasible with passive microelectrode arrays.[51,52] Apart from graphene, another carbon-based material known as carbon nanotube (CNT) has been used in μ-ECoG arrays. CNT and PDMS-based transparent stretchable electrode arrays have also been demonstrated for simultaneous electrical recording and optogenetic stimulation in rodents.[53] To leverage its phenomenal insulation property, all-silicon carbide (SiC) μ-ECoG arrays have been implemented for rodents. In such devices, the electrodes are made of doped polycrystalline SiC, which is conductive, while the insulation is composed of amorphous SiC. The seamless integration of conducting and insulating SiC layers can potentially enable extremely long-lasting device performance.[54]

It has been shown that glial cells in the brain are activated when there exists a mechanical mismatch between a foreign body and brain tissue.[55] In such cases, tissue growth is experienced around the implantable neural device causing the optical and electrical functionalities of the device to fail. This mode of failure is known as encapsulation failure and has been mostly observed and thoroughly described in chronically implanted penetrating probes. Due to their minimally invasive nature, it is generally assumed that surface arrays do not elicit such a problematic biological response, though fewer studies have been conducted on that matter. In typical dedicated studies, minimal tissue inflammation and encapsulation by collagenous scar tissue have been observed on arrays implanted subdurally in rats[56] and NHPs.[57] Another study has shown that the distribution of the tissue growth could differ depending on the array geometry after chronic implantation of μ-ECoG arrays in rat cortice.[58] This same group has also observed vascular growth around the devices.[59] Histological analysis revealed a thickening of the dura mater below the implant but no significant inflammation or glial activation after chronic implantation of an ECoG array in the cortex of a sheep.[60] To avoid encapsulation and minimize tissue response, the trend in surface array fabrication follows two common routes: use highly flexible (soft) polymer-based substrates, or adapt the array geometry, usually with ultrathin film dimensions. The goal is to obtain neural devices with similar mechanical properties to the brain tissue and maximum conformality to avoid encapsulation of the device by the brain tissue growth and achieve chronic application. The mechanical properties of the device depend on the bulk material properties as well as the geometry of the device. For example, the mechanical stiffness that characterizes the compliance of the device depends on the Young's modulus as well as the dimensions of the implantable device. Polydimethylsiloxane (PDMS) has a low Young's modulus (i.e. 1–3 MPa) among biocompatible polymers. This polymer has been used as a passive optical access port to the brain[28,61] due to its mechanical flexibility and optical transparency at the wavelengths of interest (400–700 nm). Fabricating electrodes on PDMS, however, remains a challenge due to its low surface energy, making it incompatible with traditional microfabrication techniques. In addition, its poor insulation requires additional materials in ultrathin platforms. Despite these challenges, PDMS-based neural devices have been demonstrated for neural interfacing in rodents due to the recent advancements in microfabrication techniques to define electrodes and interconnects on PDMS[12] and increase the electrode density.[62] Some of these designs and microfabrication concepts can also be translated to designing devices for NHPs. Another polymer for microfabrication is Parylene C, a transparent polymer that can be deposited using a standard chemical vapor deposition

process with control over the deposition thickness. Parylene C provides better insulation capabilities than PDMS and has been used as the substrate in several designs of neural interfaces, including high-density μ-ECoG arrays for rodents and NHPs.[23,47] The Young's modulus of Parylene C (4 GPa), however, is about three orders of magnitude larger than that of PDMS. Implementation of ultrathin films have alleviated this issue and demonstrated chronic stability in rats.[6] The third most common polymer used as a substrate is polyimide. Polyimide is compatible with commonly used fabrication processes and exhibits a high level of resistance to mechanical failure with cracks and stress. Similar to Parylene C, high-density neural probes with high electrode counts have been demonstrated in polyimide.[63] The Young's modulus of polyimide is higher than Parylene C, rendering the devices made of polyimide stiffer compared to the devices of the same dimensions made of Parylene C or PDMS. The main drawback of polyimide is its lack of optical transparency, preventing optical access to the neural tissue when used as the substrate for μ-ECoG arrays.

Devices discussed in this section have led to promising results in each area (transparency, mechanical compliance, scalability, and electrode density) but the design and fabrication of a device that incorporates all of these features remains challenging. In addition, for any device used to collect neural activity, specific neural data analysis methods must be devised, e.g., for spike sorting and feature extraction.[64] When the size of the recorded data is increased by dramatically increasing the number of recording channels or coverage, handling and analyzing such large amounts of data becomes challenging. Despite the computational challenges, the combination of the hardware level features discussed in this section will result in a μ-ECoG device that could record brain activity with high density across entire neural networks with potentially a single unit[6] and LFP oscillation-level resolution, simultaneously. Effective application of these powerful surface neural interfaces calls for the development of next-generation neural signal processing methods hand in hand with the advancements in the hardware design.

Interfaces with optical modalities

Optogenetic modulation

Although electrical stimulation has been widely used in bidirectional electric interfaces, it has limitations in terms of specificity and spatial resolution for modulating neural circuits. With the advent of optogenetics for neural stimulation,[8] new possibilities were enabled for precise and selective neuromodulation. Optogenetics is a neuromodulation technique based on the expression of microbial opsins which, when illuminated, modulate electrical activity in genetically targeted neurons. Once these light-sensitive proteins are expressed in the cell type of interest, the activity can be increased or suppressed with millisecond temporal precision by exposing the cell to light of appropriate wavelength. Optogenetics provides a unique combination of features including cell type specificity and the capacity for both excitation and inhibition of neural activity with millisecond temporal precision. It also has the potential for simultaneous interrogation of multiple brain areas without electrical artifacts, commonly observed in electrical stimulation techniques. Together, these features combine to a powerful experimental tool to study and understand how cell types, circuits, and systems operate both under normal and pathological states.

Optogenetics has been widely used in rodents to provide insights about the neural basis of behavior, physiology, or pathology.[65,66] However, small animal brains differ from primates limiting direct translation of discoveries gained from these experiments. In NHPs, optogenetics was first used to activate neurons in the primary motor cortex.[67,68] Several following studies showed that optogenetics could also be used in NHPs to link neural activity and behavior,[69–71] induce targeted plasticity in the cortex,[72] or bring new insights about different brain functions such as processing sensations[73] and mediating movement.[74] Although some rodent-specific techniques have been successfully implemented in NHPs, more developments and improvements on many different aspects are still needed for more effective and widespread optogenetic studies in NHPs.[75] First, the large size of their brain compared to that of rodents requires expressing opsins in larger volume of tissue in NHPs, thus necessitating adapted vector delivery techniques. Illuminating the large expressed area is a second challenge that requires more advanced light delivery technologies. Finally, maintaining a stable chronic optical access to large brain areas is critical for long-term optical manipulation of cortical circuits and successful functional readout coupling. These challenges are particularly relevant for optogenetic manipulation of surface cortical networks and will be discussed in the following sections. Additionally, the genetic modification and the chronic maintenance of the optical windows to these large brain areas are challenges that also apply to several optical imaging methods which are the focus of the last section.

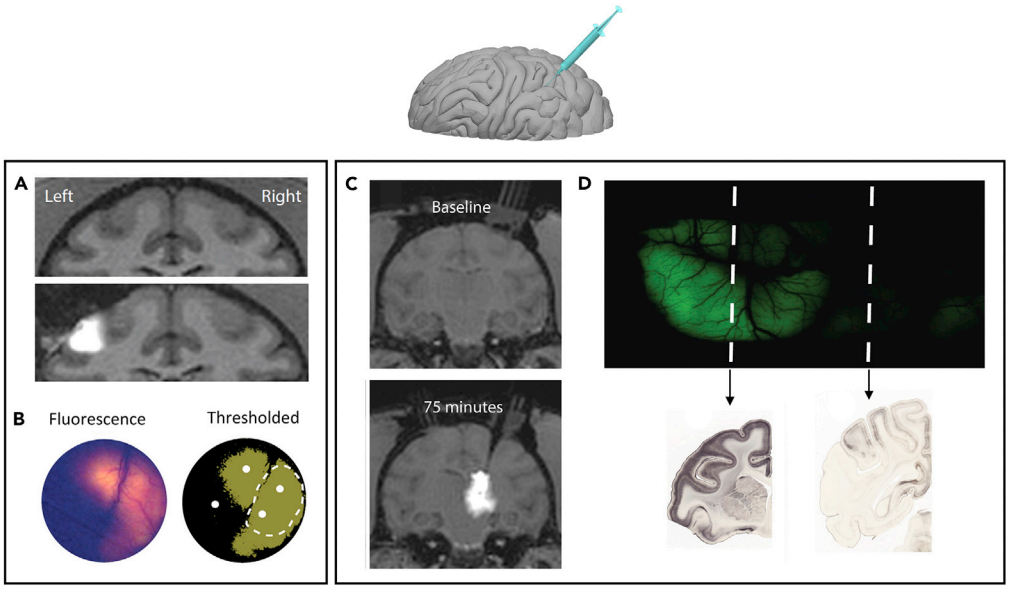

Figure 3. Genetic modification of large brain areas: convection enhanced delivery (CED) of optogenetics viral vector in NHPs

(A and B) Cortical injection. (A) Top, baseline coronal magnetic resonance (MR) image before the cortical injection of the viral vector. Bottom, spread of the virus co-infused with a contrast agent for the same MR coronal slice as in the top panel. (B) Left, epifluorescence image 3 months post infusion showing large areas of expression across somatosensory and motor cortices of a macaque. Right: epifluorescence image thresholded revealing an estimated surface area of expression of 130 mm^2. White dots indicate injection sites.

(C and D) Thalamic injection. (C) Coronal sections of real-time MR images showing the distribution volume of the viral vector co-infused with a contrast agent before (top), and 75 min after (bottom) the thalamic infusion. (D) Top, surface epifluorescent image showing the expression of the virus in the cortical areas eight weeks after the thalamic infusion. Bottom, coronal tissue sections from approximately the same sites shown with dashed lines in the top panel. YFP staining shows expression patterns consistent with the epifluorescence images in top panel. *Panels reproduced with permission from:* (A, B,[28] C, and D[81]).

Genetic modification of large brain areas. Optogenetics requires genetic modification of the targeted brain regions through the delivery of viral vectors. A key question to consider, however, is how these solution-based agents will be spread throughout large neural regions. Traditional interstitial delivery relies on diffusion from the tip of a cannula or needle inserted into the tissue, and the spread of this method is limited to volumes far smaller than the neural regions desired for large brains. To fill this technological gap, convection enhanced delivery (CED), a pressure-based approach of infusing solutions throughout large regions of the brain has been developed and utilized. In comparison with the traditional diffusion-based approach, CED achieves even distribution[76] and is roughly an order of magnitude faster than diffusion making it practical for MRI-guided techniques.[28,77–79] Additionally, CED covers roughly an order of magnitude more tissue than diffusion while reducing the number of injection sites. CED has been used to generate widespread genetic[80] and in several cases optogenetic expression in both cortical[28] (covering as much as 2 cm^2, Figures 3A and 3B) and deep structures of NHP brains[81] (Figures 3C and 3D). Importantly, CED in the thalamus has been shown to indirectly transduce even larger cortical areas than cortical CED due to thalamocortical and corticothalamic projections, albeit with reduced cortical expression density and heterogeneity among cortical layers in comparison with cortical CED[81] (Figure 3D). Of note, both of these drawbacks could be considered beneficial depending on the experimental design. Furthermore, CED has been tested both in NHPs and in humans, making it a suitable tool for genetic modification of large brains and potentially for clinical applications.[82]

Techniques for light delivery. Once the opsin of interest has been expressed in the desired brain area, different light delivery methods can be used for spatially controlled optogenetic stimulation. Using laser sources is a common option as they have a narrow spectral width that can deliver a coherent, high-intensity light at the peak activation wavelength of the opsin of interest. The low divergence of the emitted laser

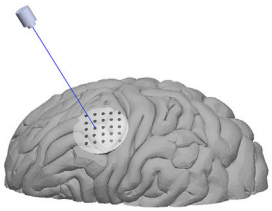

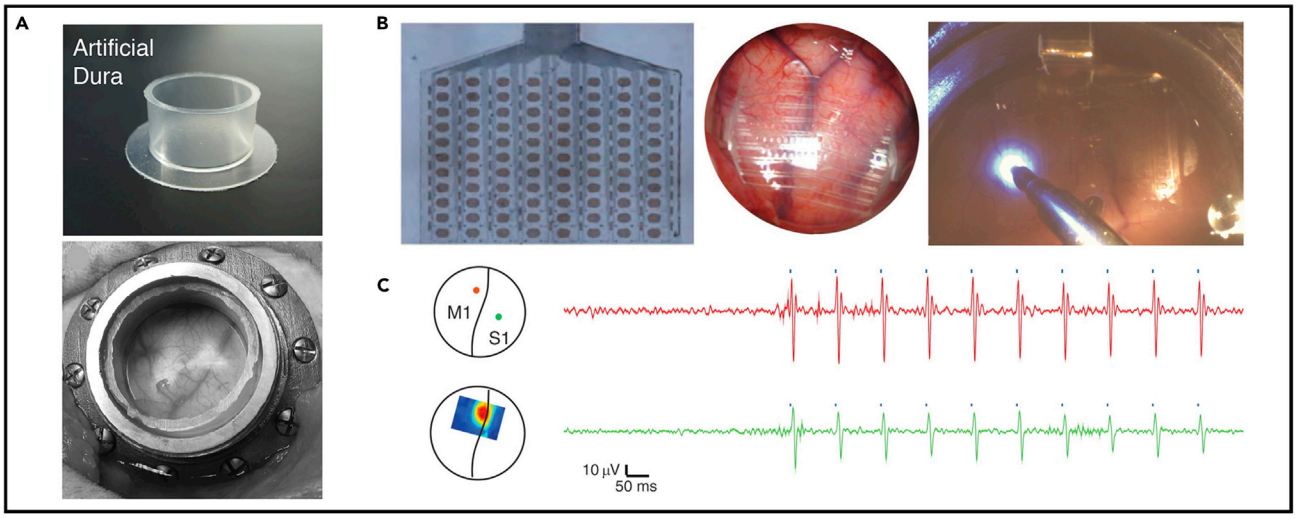

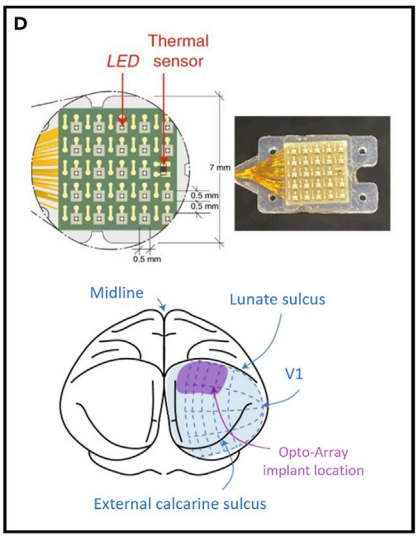

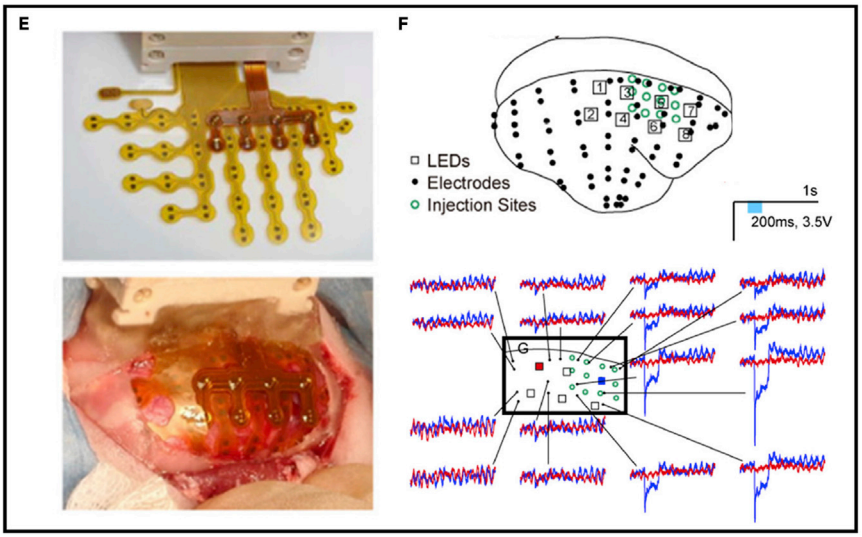

Figure 4. Strategies for large-scale surface optogenetic in NHPs

(A–C) Laser stimulation with simultaneous ECoG recording via an optical window and transparent arrays. (A) A silicone artificial dura (top) is placed in a titanium chronic chamber (bottom) as a replacement of the native dura to provide long-term optical access to motor and sensory cortices after infusion of an optogenetic viral vector. (B) 96-ch μ-ECoG array (left), two 96-ch arrays spanning motor and sensory cortices (middle), fiber optic delivering laser-pulsed light for combined optical stimulation and large-scale recording (right). (C) Example of μ-ECoG traces recorded during pulsed optical stimulation (blue ticks) from electrodes of the motor cortex (M1) (red) and from the somatosensory cortex (S1) (green) close to the respective stimulation sites shown in the top left inset. The pseudocolor map on the bottom left inset shows the spatial distribution of the high-gamma energy of evoked responses across the array for the M1 stimulation.

(D) High-density implantable LED arrays "Opto-Array" equipped with a thermal sensor (top) and chronically implanted over a macaque's primary visual cortex V1 (bottom).

(E and F) LED stimulation with simultaneous ECoG recording with opaque arrays. (E) 64-ch μ-ECoG array (yellow) and complementary shaped 8-sites LED array (red) (top) implanted on the cortical surface of a macaque monkey (bottom). (F) Top: Schematic representation of the locations of LEDs (numbered

Figure 4. *Continued*
squares), electrodes (black dots), and virus injection sites (open green circles). Bottom: example of traces recorded during photostimulation. Blue and red lines show the average waveforms of responses to LED5 in the injection area (blue square) and to LED1 in an area that was not injected (red square), respectively. *Panels reproduced with permission from:* (A–C,[28] D,[88] E, and F).[30]

beam makes them suitable for effective coupling to optical fibers. For *in vivo* optogenetic experiments, light can be directly delivered to the region of interest through fiber optics inserted into the brain. Fiber-coupled lasers were used for the first optogenetic demonstration in both rodents[83] and NHPs.[67] This method is commonly used and well established for targeting deep regions of the brain. To modulate relevant neural population adapted to their brain size, the volume of tissue to be illuminated in primates is greater than that of rodents. Optic fibers with a tapered end[84] or probes combining multiple fibers have been used to increase the illumination volume in deep regions.[85] Additionally, a fiber-coupled laser can be used to deliver light to superficial cortical areas, where no tissue penetration is required. This option has been successfully implemented in NHPs[28] (Figures 4A–4C). The fiber-coupled lasers for optogenetic manipulation of large areas in the brain are mainly limited by the number of simultaneous stimulation sites, and the bulky equipment and the large size of the fibers.[86] An appealing alternative to provide patterned stimulation modulating the activity of large areas is through LED arrays. LEDs are easy to handle and integrate as they are inexpensive and accessible. They come in a wide range of wavelengths and can be readily modulated at the intensity or frequency required without complex control electronics. LEDs can be coupled to multimode fiber optic waveguides. However, due to their highly divergent illumination profile, they have a very low coupling efficiency (~1%) that requires high-power LEDs to get a sufficient enough output power to activate the opsin of interest. Arrays comprising small LEDs are a promising alternative to optical fiber coupling as they can be directly implanted in or on the neural tissue and have the potential to illuminate large cortical areas. A recent example illustrates this possibility of use in NHPs.[87] In this study, Ohta et al. measured dopamine release via microdialysis in the prefrontal cortex following LED acute stimulation of either the prefrontal cortex (surface planar LED array) or the ventral tegmental area (linear penetrating array composed of 3 aligned LEDs) in adult male Japanese macaques. The surface LED array consisted of six rows of eight LEDs with dimensions of 9 × 6.5 mm. A second example showed behavioral perturbation during a luminance discrimination task following stimulation of the V1 area of a rhesus macaque. The LED array consisted of a 5-by-5 grid of 1-mm spaced LEDs and was chronically implanted over the cortical tissue[88] (Figure 4D). These examples illustrate the potential of LED arrays for wide-field optogenetics, as the planar matrix arrangement of multiple LEDs allows for simultaneous perturbation of large surface cortical regions. Another advantage of this array configuration is the controlled illumination of individual LEDs, or of patterns of multiple LEDs, that enables more focused perturbation of specifically targeted millimeter-scale regions. The spatial selectivity of LED can be limited by their highly divergent beam profile though making it less appealing for studies looking for cellular resolution optogenetics. Efforts to overcome this limitation include the development of smaller LEDs,[89,90] but remain to be demonstrated *in vivo* in NHPs.

Another challenge critical for directly implanted LEDs is heat management. A cortical temperature increase of 4°C can cause tissue damage and a temperature increase as low as 2°C in neural tissue can lead to significant physiological or behavioral effects.[91] To avoid unwanted effects, it is common practice to limit temperature increase of cortical tissue to 1°C.[92] While tissue heating is a consideration for any optogenetic light delivery platform, LED circuits heat up during operation, creating an additional source of temperature increase when placed at the surface of the brain. The most common method of heat management is to limit the intensity, operating time, or optical pulse length during optogenetic experiments. Thermal modeling of μ-LED arrays has shown that substrate material also influences the surface temperature of the arrays. According to these models, choosing a substrate with a lower thermal diffusivity can contribute to a lower surface temperature.[93,94] Adding a heat sink to the back of an LED array is an effective method of directing heat away from the LED array surface. Unfortunately, traditional metal heatsinks with long fins protruding away from the LED array can be challenging to incorporate into a neural interface. A potential alternative is to fabricate microstructures of a similar shape into the back of the array substrate.[95] The LED array temperature can be monitored using methods such as on-array thermal sensors,[88] (Figure 4D) thermocouple probes,[87] or thermal imagers.[49,63,96,97]

Optogenetics modulation with simultaneous ECoG readout. Combined with μ-ECoG arrays for simultaneous electrical readout, optogenetics is potentially an ideal technique for bidirectional neural interfacing, allowing for the real-time closed-loop control of neural circuits. The great advantage of closed-loop

interaction with neural circuits is the ability to deliver activity-dependent stimulation based on neural readout. O'Doherty et al.[98] have demonstrated a closed-loop brain-machine-brain interface in NHPs that controls the reaching movements of an actuator and induces artificial sensory feedback to evoke discriminable perceptions based on intracortical electrical recording and stimulation. In patients with epilepsy with the FDA-approved RNS® NeuroPace system, ECoG electrodes are used to record signals near seizure focus or foci and to electrically stimulate the targeted brain region when physician-specific patterns, such as seizures, are detected.[99] In both examples, electrical stimulation was used as the feedback mechanism as the same electrode can be used for recording and stimulation. Electrical stimulation however has associated challenges with temporal resolution and spatial specificity.[100] The use of optogenetics for neural modulation, combined with electrodes for neural recording, can mitigate the challenges associated with electrical stimulation. As mentioned in the introduction, different types of multimodal interfaces that can be used for closed-loop experiments have been demonstrated in rodents. What is more unique to μ-ECoG devices is the large area coverage and ability to record from the entire network to inform closed-loop patterned stimulation. The first *in vivo* optogenetic study combined with μ-ECoG recording was demonstrated in mice by Richner et al. in 2014.[34] In this study, cranial windowing, a surgical technique in which the skull is replaced with a small piece of cover glass was used to provide optical access to the region of interest. Cranial slits and reinforced thinned-skull windows have also been utilized as an alternative for cranial windowing techniques in rodents.[101,102] *In vivo* experiments in NHPs require μ-ECoG arrays to cover much larger surface areas. Therefore, optogenetic studies combined with μ-ECoG recording in NHPs have transitioned from a glass coverslip cranial window to a flexible and transparent silicone artificial dura that matches the curvature of large brain areas[28,47,86] (Figures 3A–3C). In this study, a transparent artificial dura was used as a replacement of the native dura to protect the brain and provide a large window of optical access. For acute experiments, the artificial dura is removed and a transparent μ-ECoG array is placed to record electrical activity during optogenetic stimulation. In this study, fiber-coupled laser is used to deliver light to the surface of the brain, and the μ-ECoG array is made with a transparent substrate to allow light to pass through with minimal attenuation. Similar strategies using transparent μ-ECoG but LED arrays instead of fiber-coupled lasers as the source of light have also been successfully implemented in rodents[49,96,103] and recently in NHPs.[104,105] A different strategy validated both in rodents[63] and NHPs[30] consists of using LEDs and μ-ECoG as two separate arrays with complementary shapes such that both can sit on the cortical surface without overlapping with each other (Figures 4E and 4F). Except for that isolated case where the ECoG array does not need to be transparent, a key challenge that most multimodal devices face is chronically maintaining the ECoG array performance and optical access to the brain for optogenetic manipulation or other optical techniques over time frames relevant to neuroscience studies, i.e., months, or ideally years.

Transparent artificial dura has been utilized since 2000 to create stable optical windows to the NHP cortex providing optical access for durations on the order of months, albeit without simultaneous ECoG recordings.[61,106–114] Artificial dura is typically protected by a cranial chamber (e.g.,[28]). In recent years, Yazdan-Shamorad et al. tested methods of combining the artificial dura with μ-ECoG arrays,[28,86] but struggled to achieve the same levels of stability achieved by ECoG-free setups. Attempts to place μ-ECoG arrays between the brain tissue and the artificial dura resulted in opaque tissue growth over the array, thus compromising the optical access after about 2–3 weeks.[86] An alternative approach where the artificial dura was temporarily explanted and the μ-ECoG array temporarily implanted for each experimental recording session resulted in accelerated tissue growth on the surface of the brain and obscured optical access after about 4 weeks.[28] In order to improve optical stability of ECoG technologies via device design, one potential avenue is to mold electrode arrays into the optical window of a traditional silicone artificial dura. Work using this approach has been recently demonstrated both acutely[33,78] and chronically.[104] In these studies, an ECoG array with electrodes made of conductive platinum particles dispersed in a transparent flexible polymer is directly molded in a silicone artificial dura.

In addition to device design, other factors can also contribute to enabling the prolonged optical access, such as the application of antibiotics to reduce the likelihood of infection, which is another important factor in chamber stability and may be correlated with optical access in some cases. For example, Shtoyerman et al. have reported that agar slows tissue regrowth[106] and that antibiotics can be mixed with agar to inhibit infection.[61,109] Roe et al. reported a protocol with routine antibiotic use which likely contributed to preventing both infection and excessive tissue growth.[110,113] Collectively, these data suggest that artificial dura and chamber maintenance protocols are important to consider where long-term experimental stability is concerned, regardless of device design.

Imaging techniques

Optical access through these large-scale chambers enables imaging the anatomy and function of the brain. Recent developments in genetically encoded tools and advanced microscopy methods have made optical techniques to monitor neural functional activity and structure very popular over the past years in small animal models such as insects or rodents. Translating these optical methods to behaving NHPs could lead to unprecedented understanding of the primate brain as it has the potential to bridge the gap between neural structure and function and provide complementary information to traditional electrophysiological monitoring. The cranial window technique using a large chronic chamber and a flexible transparent artificial dura was a key breakthrough for their adoption in NHPs as it provides the necessary large-scale optical access to the brain and the ability to accommodate the microscope objective lenses required for most imaging methods. Calcium imaging, notably, enables to visualize the activity of hundreds of individual neurons simultaneously using fluorescent calcium reporters such as dyes or genetically encoded calcium indicators (GECIs). Changes in fluorescence indicate fluctuations in intracellular calcium, which is an indirect indicator of neural activity.[7] The use of GECIs allows us to target genetically or anatomically defined neurons and to chronically record from the same population of neurons across multiple days. Calcium indicators may be limited by their kinetics, generally too slow to resolve action potentials *in vivo*. Alternatively, fluorescent voltage reporters can be used. Voltage-sensitive dyes or genetically encoded voltage indicators (GEVIs) can be used as direct reporters of cell membrane potential providing an intrinsically better temporal resolution than calcium reporters.

The use of voltage sensitive dyes in an awake behaving monkey was first demonstrated through a cranial window to map the functional organization of the cortex.[61,109] Voltage-sensitive dyes have been extensively used in NHPs to study the primary visual cortex in behaving animals.[115–117] Although GEVIs have successfully been used *in vivo* in insects[118] and rodents,[119] GEVIs generally result in signal-to-noise ratios that are lower than those resulting from GECIs.[120] Recently, significant work has been done to engineer novel variants with improved signal-to-noise ratio and spectral separation between sensors and opsins,[121] enabling all-optical stimulation and interrogation of neurons *in vivo*, in rodents.[122] Although optical imaging of membrane potential is an appealing technology for high-resolution measurements of spiking and synaptic activity in neuronal populations, their application in NHPs remains a challenge.[80] Calcium reporters on the other hand have successfully been used to precisely map the functional organization of macaque primary visual cortex in acute settings.[123,124] Additionally, GECIs have been widely used for long-term functional imaging through large cranial windows. While single-cell resolution calcium signals have been obtained with GECIs such as memTNXL,[125] GCaMP-family is the most extensively used kind of calcium indicator. Wide-field single-photon imaging has been successfully used to image GCaMP in the primary visual cortex of awake macaques.[112] GCaMP-based calcium imaging using two-photon microscopy is the most common configuration and it has enabled functional imaging of various cortical regions including neocortex,[126] somatosensory cortex,[127] visual cortex,[128] and motor cortex.[129,130] Recent interest in motor cortex imaging has been motivated by the promises of optical brain computer interfaces[130] (Figures 5A–5C). In this study, Trautmann et al. developed a dedicated chronic cranial chamber (Figure 5A) to accommodate 2P calcium imaging (Figure 5B) in combination with a structural imaging technique (Figure 5C). With this system, they were able to image large populations of neurons in the motor cortex and successfully decode movement from the dendritic signals they obtained. Another example combining multiple functional imaging techniques have been recently demonstrated.[131] In that study, two-photon calcium imaging and intrinsic optical signal imaging were consecutively used in the same subject to precisely define the tonotopic map of the primary auditory cortex. These studies illustrate the potential of multi-technique optical interfaces.

Functional imaging is also a powerful technique as a readout method to measure the evoked activity in response to optogenetics manipulation of cortical circuits. One of the major challenges of this all-optical interrogation concept is the overlapping absorption wavelength band (i.e. blue light) of GECIs and the most commonly used opsin, ChR2. This challenge can be addressed with the use of red-shifted excitatory opsins that allow better spectral separation between the excitation light used to image activity and the stimulation light used to activate the opsin, thus reducing unwanted cross-talk stimulation.[132] Optogenetic stimulation with simultaneous calcium imaging readout in the same optical window was first demonstrated in 2014 in awake behaving mice using the red-shifted opsin C1V1 and GCaMP3 as the calcium sensor.[133] Other red-shifted opsins have been developed and implemented in rodents such as ChRmine[134] or bReaChES[135] and researchers are actively engineering novel variants,[136] contributing to

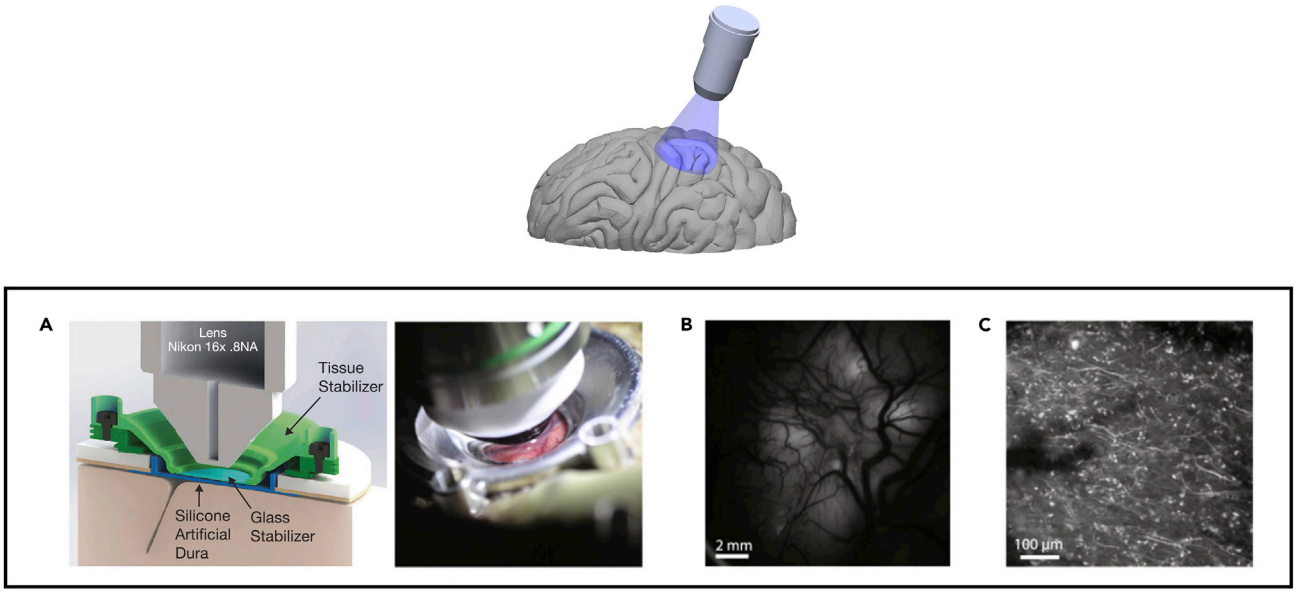

Figure 5. Combined functional and structural imaging

(A) Schematic (left) and photography (right) of the imaging set-up used for structural and functional imaging: a titanium chamber and a silicone artificial dura are chronically implanted to provide imaging access to a 12-mm diameter region of premotor and motor cortex using an objective lens.

(B) Widefield 1P image of microvasculature of the cortical area within the chamber. In this study, it was used to assess expression of genetically encoded calcium reporter and to establish vasculature markers for navigating to specific sites of the cortex.

(C) Two-photon Ca^{2+} image showing single-cell resolution functional signals from motor cortex. *Panels reproduced from.*[130]

make this all optical interrogation concept increasingly popular in rodents. In NHPs, while work by Sengupta et al. had demonstrated the practical use of red-shifted opsins (ReaChR) in a macaque's retina in 2016,[137] it was not before 2018 that Ju et al. demonstrated two-photon calcium imaging with simultaneous optogenetic stimulation in the primary visual cortex (V1) of awake macaque monkeys, using C1V1 and GCaMP5/GCaMP6[138] (Figures 6A–6C). Before that, pioneer work by Ruiz et al. in 2013 had shown combined optogenetics with both *in vivo* epifluorescence imaging and optical intrinsic signal imaging.[113]

Despite the huge potential of functional imaging techniques as readout methods, significant challenges remain for their widespread use, notably in terms of two-photon performances, image acquisition process (motion of the brain relative to the objective lens that require stabilization techniques to limit artifacts, longevity of optical access, etc.), as well as image analysis process (identifying neurons, spike detection etc). The potential and challenges of functional imaging techniques such as voltage or calcium imaging in NHPs have been more extensively discussed elsewhere.[139]

Another way to obtain valuable information about the brain with optical techniques is through vascular imaging which can provide both structural and hemodynamic information. Optical coherence tomography angiography (OCTA), notably, is a non-invasive approach that can visualize blood vessels down to the capillary level. While OCTA has been widely used for ophthalmology applications because of its successful implementation in the retina, it has also been used in rodents to study traumatic brain injury, cerebral stroke, and brain aging.[140] In NHPs, OCTA has been used in stroke model studies to image large-scale cortical vascular dynamics, confirming the location and size of induced ischemic lesions[141–144] (Figure 7A). OCTA imaging through a semi-transparent μ-ECoG array has also been demonstrated, revealing blood flow images obstructed only by the non-transparent electrodes and traces[33] (Figure 7B). In this study, the successful implementation of OCTA imaging in combination with electrophysiology recordings was permitted by the transparency of the array, suggesting that these large-scale interfaces could incorporate other optical techniques such as optogenetics and calcium imaging. This latest study and others described earlier in this review demonstrate the great potential of combining multiple optical and/or electrical techniques within the same large-scale interfaces. We believe that multifunctional neural interfaces combining existing approaches will revolutionize our understanding of the NHP brain.

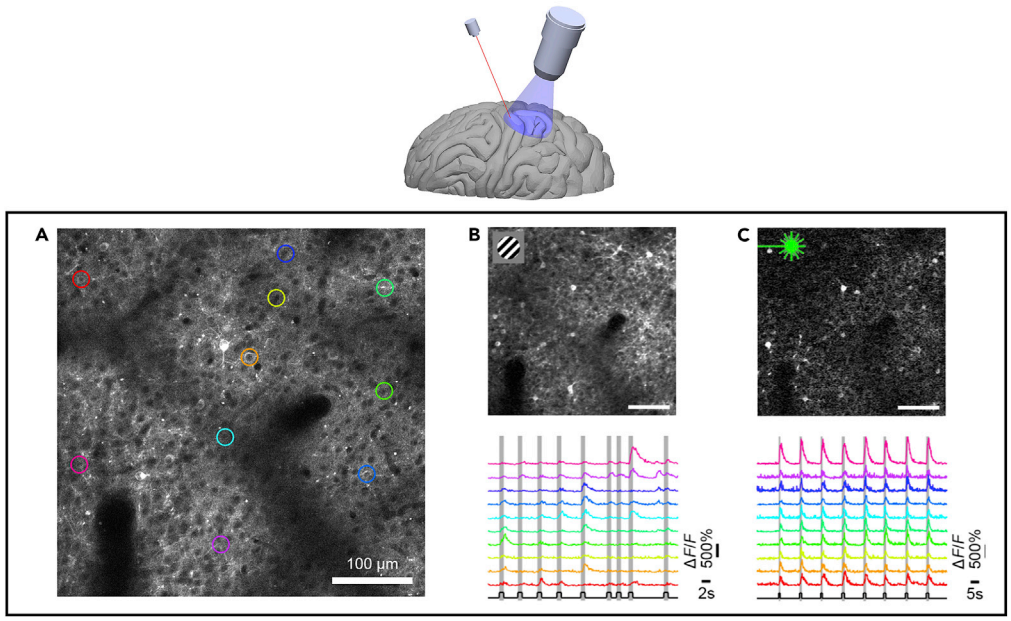

Figure 6. Optogenetic stimulation with simultaneous functional imaging readout

(A) Two-photon image of neurons from the visual cortex (V1) expressing a genetically encoded calcium indicator (GCaMP). The colored regions of interest (ROIs) indicate neurons that responded to both visual and optical stimuli in panel (B and C), respectively.

(B) Top: a differential fluorescence image (stimulated (F) – baseline (F0)) driven by visual stimuli consisting of gratings patches (inset). Bottom, calcium signals from 10 neurons (colors from panel (A)) in response to 9 varied visual stimuli (presentation times in gray).

(C) Top, widefield optogenetic stimulation evoked responses in the same neurons. Bottom, 8 sequential identical optogenetic stimulations evoked equivalent responses. *Panels reproduced from.*[138]

CONCLUDING REMARKS

Neural interfaces with electrical and optical capabilities are powerful tools to study and understand the mechanisms of brain functions. Developing such neural interfaces for NHPs is essential to bridge the gap between state-of-the-art rodent studies and clinical applications.

In this work, we reviewed the latest development in electrical and optical interfaces for large-scale neural activity recording and stimulation in NHPs, and we discussed the challenges of conducting such experiments in these large animals. Some state-of-the-art materials and design strategies now commonly used for rodent interfaces have been successfully implemented in NHP interfaces. Flexible polymers, for example, proved effective for μ-ECoG large surface coverage, revealing a good compliance with the brain, and advances in CMOS fabrication technologies allowed significant improvement of the number of recording and stimulation channels and electrode density. Further scaling up the number of recording and modulation sites as well as the overall surface coverage is undoubtedly the trend in μ-ECoG technology to achieve operation with high spatiotemporal resolution and cover multiple brain areas in large brains. While multiplexing has proven to be a useful strategy to connect large numbers of electrodes, innovations would still be required to improve the back-end electronics and connectors required for high channel count recordings. Wireless transmission of data and power would allow for a fully implantable form factor and promise a great future for next-generation μ-ECoG technologies. Surface μ-ECoG arrays used in tandem with optical stimulation and imaging techniques present a useful addition to the neuroscience toolset and provide a great opportunity to dissect the functions of neural circuits with different origins and at different scales. The development of partially optically clear arrays enabled simultaneous recording of cortical activity and neural stimulation via optogenetics. Functional imaging techniques have also proven to be great candidates to be combined with optogenetics as readout methods for all optical control and readout of cortical circuits, or with other imaging techniques providing complementary structural or hemodynamic information such as OCTA. Combining these advanced optical imaging modalities with optogenetics and electrical recording offers exciting opportunities to

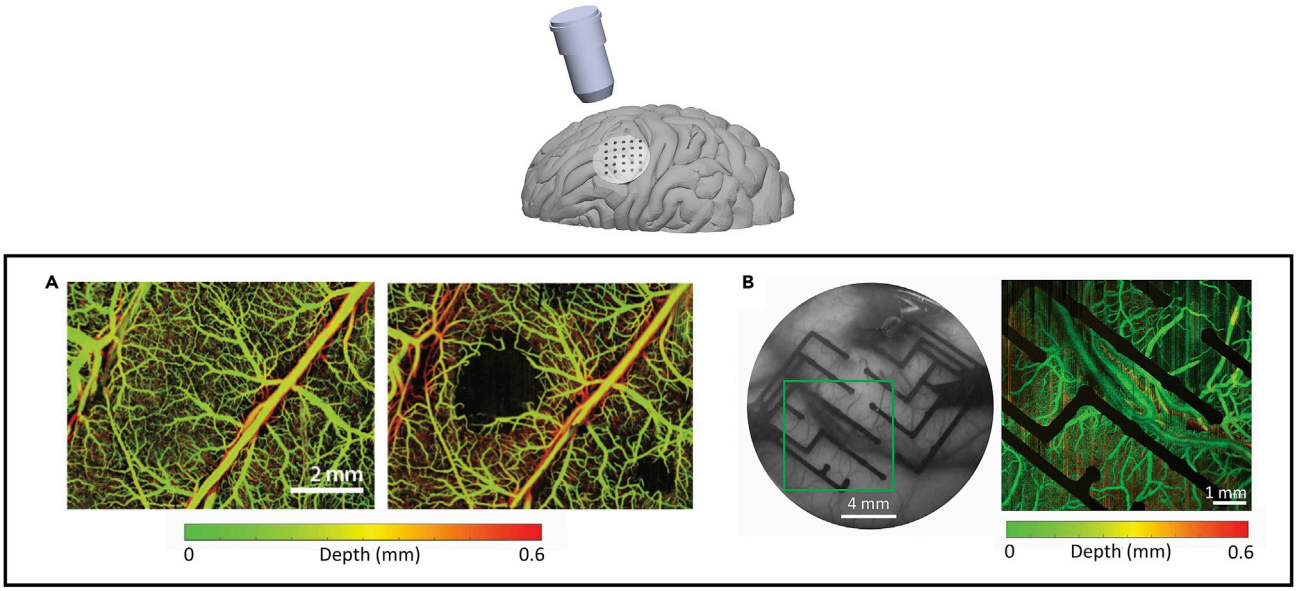

Figure 7. Combined large-scale ECoG recording and structural imaging

(A) *In vivo* optical coherence tomography (OCTA) images showing the microvasculature of the sensorimotor cortex of a macaque before (top) and 3 h after (bottom) inducing a focal ischemic lesion (stroke).

(B) Grayscale picture of a μ-ECoG array on the sensorimotor cortex of an NHP (left). Green box indicates the region imaged on the right panel. OCTA of the cortex as imaged through the array (right). *Panels reproduced with permission from* (A[141] and B[33]).

interrogate and explore the relationship between electrophysiology, cellular metabolism, or vascular dynamics. We foresee that multifunctional neural interfaces combining multiple existing approaches could revolutionize our understanding of the brain. Using advanced multimodal neural interfaces to study brain in NHPs models that are close to humans from an evolutionary point of view and that can be trained to perform cognitively sophisticated tasks could lead to new powerful ways to study and understand the healthy and diseased nervous system. The growing set of neurotechnological tools available to NHP researchers could drive the development of future rehabilitative therapies for stroke, traumatic brain injury, and other neurological disorders.

PERSPECTIVE ON ETHICS CONSIDERATIONS: PROTECTIONS FOR NHPS AND CHALLENGES OF TRANSLATIONAL NEUROSCIENCE

The arguably greatest potential benefit of large-scale optical and μ-ECoG imaging and stimulation in NHPs is the rapid expansion of neuroscientific knowledge that could translate to human models and drive the development of restorative therapies. However, the invasive procedures required for chronic, real-time recording and manipulation that would be useful for translation to human models raise logistical challenges for maintaining the wellbeing of nonhuman animals (NHAs) within studies.[145] Progress toward improved therapeutic practices in humans through research on NHP requires careful evaluation of the treatment of NHPs (and other NHAs) within studies alongside the prospect of translating insights gained from those studies to insights about human models.

Treatment of NHAs in neuroscientific research is guided in part by the "3Rs" framework originally proposed by Russell and Burch.[146] This framework calls on investigators to *replace* sentient animals with "less sentient" animals whenever possible, *reduce* the number of animals used in studies, and *refine* study procedures to minimize the amount of distress animals experience. Several scientists have called for refinements to how the 3Rs are implemented into neuroscientific practice, calling for greater accountability to rationales for research, richer cultures of animal welfare, and more oversight from public institutions governing translational medicine.[147] Others recommend that we add to three more "Rs" to the 3Rs framework, arguing that researchers have ethical obligations to strive toward more *robust* study design, *registration* of NHA studies for the sake of public and scientific scrutiny, and improved *reporting* of both positive and negative results.[148]

Studies using large-scale, chronic neural recording techniques must make the most of recorded data to justify any actual or potential distress caused to NHAs during studies. The implementation of FAIR—findable, accessible, interoperable, and reproducible—practices for handling and distributing neurophysiological data are an important necessity in this context. For example, data standards like Neurodata Without Borders[149] as well as long-term repositories like the Distributed Archives for Neurophysiology Data Integration, OpenNeuro,[150] and the PRIMatE Data Exchange[151,152] would allow researchers to reuse data from, increase the impact of, and reduce the number of NHP (and all NHA) studies.

Several ethical problems arise from the transition from animal models to human models. To translate research using animal models to human models, investigators must design studies using close human analogs, including NHPs. 3Rs-style guidance to replace NHPs with less sentient NHAs, however, stands in tension with the goal of translating neuroscientific discoveries into therapeutic practices. This leads to a *justificatory dilemma*: the use of NHPs (over other NHAs) on the basis of their similarity to humans stands in tension with the intuition that humans deserve more moral consideration than NHPs.[153] This tension is eased by the prospect of using long-term or chronic recording techniques to produce more robust data in rich experimental contexts with fewer NHPs (and other NHAs) required. However, the data scientific practices that are well suited to making the most of NHP research will likely raise further ethical considerations when applied to human subject research.[154,155] Users of therapeutic and assistive devices resulting from or enabled by large-scale neural recordings will likely face issues related to the impact of neurotechnology on agency, especially with respect to parsing out their responsibility for neurotech-assisted actions, trusting their device to function in ways that line up with their interests, keeping their neural activity private, and the impact of neurotech on their feelings of authentic self-hood.[156] For instance, human participants will likely have worries about harmful or spurious uses of their neural data and may want the option to remove their data from public repositories and future studies.

ACKNOWLEDGMENTS

This work was supported by the National Institute of Health NIH 5R01NS116464 (T.B., S.M.-V., M.C., and A.Y.-S.), NIH T32 EB029365 (S.M.-V.), NIH R01 NS119395 (D.J.G.), NIH 1RF1NS113303 (M.C.), the National Science Foundation NSF 1926804 (M.C.), the Washington National Primate Research Center (WaNPRC, NIH P51 OD010425, U42 OD011123) and Weill Neurohub (S.F.).

AUTHOR CONTRIBUTIONS

Conceptualization, T.B. and A.Y.; Investigation, T.B., S.M.-V., Z.A., D.J.G., S.F., and T.B.; Writing-Original Draft, T.B., S.M.-V., Z.A., D.J.G., S.F., and T.B.; Writing-Review & Editing, T.B., S.M.-V., M.C., and A.Y.; Visualization, T.B.; Funding Acquisition, M.C. and A.Y.; Supervision, M.C. and A.Y.

DECLARATION OF INTERESTS

The authors declare no competing interest.

INCLUSION AND DIVERSITY

One or more of the authors of this paper self-identifies as an underrepresented ethnic minority in their field of research or within their geographical location. One or more of the authors of this paper self-identifies as a gender minority in their field of research. One or more of the authors of this paper self-identifies as living with a disability. While citing references scientifically relevant for this work, we also actively worked to promote gender balance in our reference list.

REFERENCES

1. Steinmetz, N.A., Aydin, C., Lebedeva, A., Okun, M., Pachitariu, M., Bauza, M., Beau, M., Bhagat, J., Böhm, C., Broux, M., et al. (2021). Neuropixels 2.0: a miniaturized high-density probe for stable, long-term brain recordings. Science *372*. eabf4588. https://doi.org/10.1126/SCIENCE.ABF4588/.

2. Fu, T.M., Hong, G., Viveros, R.D., Zhou, T., and Lieber, C.M. (2017). Highly scalable multichannel mesh electronics for stable chronic brain electrophysiology. Proc. Natl. Acad. Sci. USA *114*, E10046–E10055. https://doi.org/10.1073/PNAS.1717695114/.

3. Fiáth, R., Hofer, K.T., Csikós, V., Horváth, D., Nánási, T., Tóth, K., Pothof, F., Böhler, C., Asplund, M., Ruther, P., et al. (2018). Long-term recording performance and biocompatibility of chronically implanted cylindrically-shaped, polymer-based neural interfaces. Biomed. Tech. *63*, 301–315. https://doi.org/10.1515/BMT-2017-0154/.

4. Meng, J., Zhang, S., Bekyo, A., Olsoe, J., Baxter, B., and He, B. (2016). Noninvasive electroencephalogram based control of a robotic arm for reach and grasp tasks. Sci. Rep. *6*, 38565. https://doi.org/10.1038/srep38565.

5. Shokoueinejad, M., Park, D.W., Jung, Y.H., Brodnick, S.K., Novello, J., Dingle, A., Swanson, K.I., Baek, D.H., Suminski, A.J., Lake, W.B., et al. (2019). Progress in the field of micro-electrocorticography. Micromachines *10*, 62. https://doi.org/10.3390/mi10010062.

6. Khodagholy, D., Gelinas, J.N., Thesen, T., Doyle, W., Devinsky, O., Malliaras, G.G., and Buzsáki, G. (2015). NeuroGrid: recording action potentials from the surface of the brain. Nat. Neurosci. *18*, 310–315. https://doi.org/10.1038/nn.3905.

7. Grienberger, C., and Konnerth, A. (2012). Imaging calcium in neurons. Neuron *73*, 862–885. https://doi.org/10.1016/j.neuron.2012.02.011.

8. Boyden, E.S., Zhang, F., Bamberg, E., Nagel, G., and Deisseroth, K. (2005). Millisecond-timescale, genetically targeted optical control of neural activity. Nat. Neurosci. *8*, 1263–1268. https://doi.org/10.1038/nn1525.

9. Kim, K., Vöröslakos, M., Seymour, J.P., Wise, K.D., Buzsáki, G., and Yoon, E. (2020). Artifact-free and high-temporal-resolution in vivo opto-electrophysiology with microLED optoelectrodes. Nat. Commun. *11*, 2063. https://doi.org/10.1038/s41467-020-15769-w.

10. Reddy, J.W., Kimukin, I., Stewart, L.T., Ahmed, Z., Barth, A.L., Towe, E., and Chamanzar, M. (2019). High density, double-sided, flexible optoelectronic neural probes with embedded μLEDs. Front. Neurosci. *13*, 745. https://doi.org/10.3389/FNINS.2019.00745/BIBTEX.

11. Park, D.W., Schendel, A.A., Mikael, S., Brodnick, S.K., Richner, T.J., Ness, J.P., Hayat, M.R., Atry, F., Frye, S.T., Pashaie, R., et al. (2014). Graphene-based carbon-layered electrode array technology for neural imaging and optogenetic applications. Nat. Commun. *5*, 5258. https://doi.org/10.1038/ncomms6258.

12. Renz, A.F., Lee, J., Tybrandt, K., Brzezinski, M., Lorenzo, D.A., Cerra Cheraka, M., Lee, J., Helmchen, F., Vörös, J., and Lewis, C.M. (2020). Opto-E-dura: a soft, stretchable ECoG array for multimodal, multiscale neuroscience. Adv. Healthc. Mater. *9*. 2000814. https://doi.org/10.1002/ADHM.202000814.

13. Ahmed, Z., Reddy, J.W., Malekoshoaraie, M.H., Hassanzade, V., Kimukin, I., Jain, V., and Chamanzar, M. (2021). Flexible optoelectric neural interfaces. Curr. Opin. Biotechnol. *72*, 121–130. https://doi.org/10.1016/J.COPBIO.2021.11.001.

14. Vázquez-Guardado, A., Yang, Y., Bandodkar, A.J., and Rogers, J.A. (2020). Recent advances in neurotechnologies with broad potential for neuroscience research. Nat. Neurosci. *23*, 1522–1536. https://doi.org/10.1038/S41593-020-00739-8.

15. Ramezani, Z., Seo, K.J., and Fang, H. (2021). Hybrid electrical and optical neural interfaces. J. Micromech. Microeng. *31*, 044002. https://doi.org/10.1088/1361-6439/abeb30.

16. Sung, C., Jeon, W., Nam, K.S., Kim, Y., Butt, H., and Park, S. (2020). Multimaterial and multifunctional neural interfaces: from surface-type and implantable electrodes to fiber-based devices. J. Mater. Chem. B *8*, 6624–6666. https://doi.org/10.1039/d0tb00872a.

17. Nurmikko, A. (2020). Challenges for large-scale cortical interfaces. Neuron *108*, 259–269. https://doi.org/10.1016/j.neuron.2020.10.015.

18. Yazdan-shahmorad, A., Silversmith, D.B., and Sabes, P.N. (2018). Novel techniques for large-scale manipulations of cortical networks in non-human primates. 2018 40th. Annu. Int. Conf. IEEE Eng. Med. Biol. Soc. *2018*, 5479–5482.

19. Bloch, J.A., Khateeb, K., Silversmith, D.B., O'Doherty, J.E., Sabes, P.N., and Yazdan-Shahmorad, A. (2019). Cortical stimulation induces network-wide coherence change in non-human primate somatosensory cortex. Annu. Int. Conf. IEEE Eng. Med. Biol. Soc. *2019*, 6446–6449. https://doi.org/10.1109/EMBC.2019.8856633.

20. Bloch, J., Greaves-Tunnell, A., Shea-Brown, E., Harchaoui, Z., Shojaie, A., and Yazdan-Shahmorad, A. (2022). Network structure mediates functional reorganization induced by optogenetic stimulation of non-human primate sensorimotor cortex. iScience *25*, 104285. https://doi.org/10.1016/J.ISCI.2022.104285.

21. Buzsáki, G., Anastassiou, C.A., and Koch, C. (2012). The origin of extracellular fields and currents — EEG, ECoG, LFP and spikes. Nat. Rev. Neurosci. *13*, 407–420. https://doi.org/10.1038/nrn3241.

22. Chiang, C.H., Won, S.M., Orsborn, A.L., Yu, K.J., Trumpis, M., Bent, B., Wang, C., Xue, Y., Min, S., Woods, V., et al. (2020). Development of a neural interface for high-definition, long-term recording in rodents and nonhuman primates. Sci. Transl. Med. *12*. eaay4682. https://doi.org/10.1126/scitranslmed.aay4682.

23. Kaiju, T., Inoue, M., Hirata, M., and Suzuki, T. (2021). High-density mapping of primate digit representations with a 1152-channel μECoG array. J. Neural. Eng. *18*, 036025. https://doi.org/10.1088/1741-2552/abe245.

24. Song, E., Chiang, C.H., Li, R., Jin, X., Zhao, J., Hill, M., Xia, Y., Li, L., Huang, Y., Won, S.M., et al. (2019). Flexible electronic/optoelectronic microsystems with scalable designs for chronic biointegration. Proc. Natl. Acad. Sci. USA *116*, 15398–15406. https://doi.org/10.1073/PNAS.1907697116/.

25. Hermiz, J., Hossain, L., Arneodo, E.M., Ganji, M., Rogers, N., Vahidi, N., Halgren, E., Gentner, T.Q., Dayeh, S.A., and Gilja, V. (2020). Stimulus driven single unit activity from micro-electrocorticography. Front. Neurosci. *14*, 55. https://doi.org/10.3389/fnins.2020.00055.

26. Rubehn, B., Bosman, C., Oostenveld, R., Fries, P., and Stieglitz, T. (2009). A MEMS-based flexible multichannel ECoG-electrode array. J. Neural. Eng. *6*, 036003. https://doi.org/10.1088/1741-2560/6/3/036003.

27. Thongpang, S., Richner, T.J., Brodnick, S.K., Schendel, A., Kim, J., Wilson, J.A., Hippensteel, J., Krugner-Higby, L., Moran, D., Ahmed, A.S., et al. (2011). A micro-electrocorticography platform and deployment strategies for chronic BCI applications. Clin. EEG Neurosci. *42*, 259–265. https://doi.org/10.1177/155005941104200412.

28. Yazdan-Shahmorad, A., Diaz-Botia, C., Hanson, T.L., Kharazia, V., Ledochowitsch, P., Maharbiz, M.M., and Sabes, P.N. (2016). A large-scale interface for optogenetic stimulation and recording in nonhuman primates. Neuron *89*, 927–939. https://doi.org/10.1016/j.neuron.2016.01.013.

29. Kaiju, T., Doi, K., Yokota, M., Watanabe, K., Inoue, M., Ando, H., Takahashi, K., Yoshida, F., Hirata, M., and Suzuki, T. (2017). High spatiotemporal resolution ECoG recording of somatosensory evoked potentials with flexible micro-electrode arrays. Front. Neural Circuits *11*, 20. https://doi.org/10.3389/fncir.2017.00020.

30. Komatsu, M., Sugano, E., Tomita, H., and Fujii, N. (2017). A chronically implantable bidirectional neural interface for non-human primates. Front. Neurosci. *11*, 514. https://doi.org/10.3389/fnins.2017.00514.

31. Miyakawa, N., Majima, K., Sawahata, H., Kawasaki, K., Matsuo, T., Kotake, N., Suzuki, T., Kamitani, Y., and Hasegawa, I. (2018). Heterogeneous redistribution of facial subcategory information within and outside the face-selective domain in primate inferior temporal cortex. Cereb. Cortex *28*, 1416–1431. https://doi.org/10.1093/cercor/bhx342.

32. Chiang, C.-H., Lee, J., Wang, C., Williams, A.J., Lucas, T.H., Cohen, Y.E., and Viventi, J. (2020). A modular high-density μECoG system on macaque vlPFC for auditory cognitive decoding. J. Neural. Eng. *17*, 046008. https://doi.org/10.1088/1741-2552/ab9986.

33. Griggs, D.J., Khateeb, K., Zhou, J., Liu, T., Wang, R., and Yazdan-Shahmorad, A. (2021). Multi-modal artificial dura for simultaneous large-scale optical access and large-scale electrophysiology in non-human primate cortex. J. Neural. Eng. *18*, 055006. https://doi.org/10.1088/1741-2552/abf28d.

34. Richner, T.J., Thongpang, S., Brodnick, S.K., Schendel, A.A., Falk, R.W., Krugner-Higby, L.A., Pashaie, R., and Williams, J.C. (2014). Optogenetic micro-electrocorticography for modulating and localizing cerebral cortex activity. J. Neural. Eng. *11*, 016010. https://doi.org/10.1088/1741-2560/11/1/016010.

35. Rogers, N., Hermiz, J., Ganji, M., Kaestner, E., Kılıç, K., Hossain, L., Thunemann, M., Cleary, D.R., Carter, B.S., Barba, D., et al. (2019). Correlation structure in micro-ECoG

recordings is described by spatially coherent components. PLoS Comput. Biol. *15*, e1006769. https://doi.org/10.1371/journal.pcbi.1006769.

36. Chang, E.F. (2015). Towards large-scale, human-based, mesoscopic neurotechnologies. Neuron *86*, 68–78. https://doi.org/10.1016/j.neuron.2015.03.037.

37. Worrell, G.A., Jerbi, K., Kobayashi, K., Lina, J.M., Zelmann, R., and Le Van Quyen, M. (2012). Recording and analysis techniques for high-frequency oscillations. Prog. Neurobiol. *98*, 265–278. https://doi.org/10.1016/j.pneurobio.2012.02.006.

38. Huang, X., Londono-Ramirez, H., Ballini, M., Van Hoof, C., Genoe, J., Haesler, S., Gielen, G., Helleputte, N.V., and Lopez, C.M. (2022). Actively multiplexed μECoG brain implant system with incremental-ΔΣ ADCs employing bulk-DACs. IEEE J. Solid State Circuits *57*, 3312–3323. https://doi.org/10.1109/JSSC.2022.3201704.

39. Castagnola, E., Maiolo, L., Maggiolini, E., Minotti, A., Marrani, M., Maita, F., Pecora, A., Angotzi, G.N., Ansaldo, A., Boffini, M., et al. (2015). Pedot-cnt-coated low-impedance, ultra-flexible, and brain-conformable micro-ECoG arrays. IEEE Trans. Neural Syst. Rehabil. Eng. *23*, 342–350. https://doi.org/10.1109/TNSRE.2014.2342880.

40. Schander, A., Strokov, S., Stemmann, H., Tebmann, T., Kreiter, A.K., and Lang, W. (2019). A flexible 202-channel epidural ECoG array with PEDOT: PSS coated electrodes for chronic recording of the visual cortex. IEEE Sensors J. *19*, 820–825. https://doi.org/10.1109/JSEN.2018.2880833.

41. Khodagholy, D., Doublet, T., Gurfinkel, M., Quilichini, P., Ismailova, E., Leleux, P., Herve, T., Sanaur, S., Bernard, C., and Malliaras, G.G. (2011). Highly conformable conducting polymer electrodes for in vivo recordings. Adv. Mater. *23*, 268–272. https://doi.org/10.1002/adma.201102378.

42. Driscoll, N., Richardson, A.G., Maleski, K., Anasori, B., Adewole, O., Lelyukh, P., Escobedo, L., Cullen, D.K., Lucas, T.H., Gogotsi, Y., and Vitale, F. (2018). Two-dimensional Ti3C2 MXene for high-resolution neural interfaces. ACS Nano *12*, 10419–10429. https://doi.org/10.1021/acsnano.8b06014.

43. Fan, B., Rodriguez, A.V., Vercosa, D.G., Kemere, C., and Robinson, J.T. (2020). Sputtered porous Pt for wafer-scale manufacture of low-impedance flexible microelectrodes. J. Neural. Eng. *17*, 036029. https://doi.org/10.1088/1741-2552/ab965c.

44. Vomero, M., Zucchini, E., Delfino, E., Gueli, C., Mondragon, N.C., Carli, S., et al. (2018). Glassy carbon electrocorticography electrodes on Ultra-Thin and Finger-Like Polyimide Substrate: performance evaluation based on different electrode diameters. Materials *11*, 2486. https://doi.org/10.3390/ma11122486.

45. Vomero, M., Castagnola, E., Ciarpella, F., Maggiolini, E., Goshi, N., Zucchini, E., Carli, S., Fadiga, L., Kassegne, S., and Ricci, D. (2017). Highly stable glassy carbon interfaces for long-term neural stimulation and low-noise recording of brain activity. Sci. Rep. *7*, 40332. https://doi.org/10.1038/srep40332.

46. Ledochowitsch, P., Olivero, E., Blanche, T., and Maharbiz, M.M. (2011). A transparent ECoG array for simultaneous recording and optogenetic stimulation. Annu. Int. Conf. IEEE Eng. Med. Biol. Soc. *2011*, 2937–2940. https://doi.org/10.1109/IEMBS.2011.6090808.

47. Ledochowitsch, P., Yazdan-Shahmorad, A., Bouchard, K.E., Diaz-Botia, C., Hanson, T.L., He, J.W., Seybold, B.A., Olivero, E., Phillips, E.A.K., Blanche, T.J., et al. (2015). Strategies for optical control and simultaneous electrical readout of extended cortical circuits. J. Neurosci. Methods *256*, 220–231. https://doi.org/10.1016/j.jneumeth.2015.07.028.

48. Jimbo, Y., Matsuhisa, N., Lee, W., Zalar, P., Jinno, H., Yokota, T., Sekino, M., and Someya, T. (2017). Ultraflexible transparent oxide/metal/oxide stack electrode with low sheet resistance for electrophysiological measurements. ACS Appl. Mater. Interfaces *9*, 34744–34750. https://doi.org/10.1021/acsami.7b12802.

49. Kwon, K.Y., Sirowatka, B., Weber, A., and Li, W. (2013). Opto-μ ECoG array: a hybrid neural interface with transparent μ ECoG electrode array and integrated LEDs for optogenetics. IEEE Trans. Biomed. Circuits Syst. *7*, 593–600. https://doi.org/10.1109/TBCAS.2013.2282318.

50. Kuzum, D., Takano, H., Shim, E., Reed, J.C., Juul, H., Richardson, A.G., de Vries, J., Bink, H., Dichter, M.A., Lucas, T.H., et al. (2014). Transparent and flexible low noise graphene electrodes for simultaneous electrophysiology and neuroimaging. Nat. Commun. *5*, 5259. https://doi.org/10.1038/ncomms6259.

51. Masvidal-Codina, E., Illa, X., Dasilva, M., Calia, A.B., Dragojević, T., Vidal-Rosas, E.E., Prats-Alfonso, E., Martínez-Aguilar, J., De la Cruz, J.M., Garcia-Cortadella, R., et al. (2019). High-resolution mapping of infraslow cortical brain activity enabled by graphene microtransistors. Nat. Mater. *18*, 280–288. https://doi.org/10.1038/s41563-018-0249-4.

52. Garcia-Cortadella, R., Schwesig, G., Jeschke, C., Illa, X., Gray, A.L., Savage, S., Stamatidou, E., Schiessl, I., Masvidal-Codina, E., Kostarelos, K., et al. (2021). Graphene active sensor arrays for long-term and wireless mapping of wide frequency band epicortical brain activity. Nat. Commun. *12*, 211. https://doi.org/10.1038/s41467-020-20546-w.

53. Zhang, J., Liu, X., Xu, W., Luo, W., Li, M., Chu, F., Xu, L., Cao, A., Guan, J., Tang, S., and Duan, X. (2018). Stretchable transparent electrode arrays for simultaneous electrical and optical interrogation of neural circuits in vivo. Nano Lett. *18*, 2903–2911. https://doi.org/10.1021/acs.nanolett.8b00087.

54. Diaz-Botia, C.A., Luna, L.E., Neely, R.M., Chamanzar, M., Carraro, C., Carmena, J.M., Sabes, P.N., Maboudian, R., and Maharbiz, M.M. (2017). A silicon carbide array for electrocorticography and peripheral nerve recording. J. Neural. Eng. *14*, 056006. https://doi.org/10.1088/1741-2552/aa7698.

55. Moshayedi, P., Ng, G., Kwok, J.C.F., Yeo, G.S.H., Bryant, C.E., Fawcett, J.W., Franze, K., and Guck, J. (2014). The relationship between glial cell mechanosensitivity and foreign body reactions in the central nervous system. Biomaterials *35*, 3919–3925. https://doi.org/10.1016/j.biomaterials.2014.01.038.

56. Henle, C., Raab, M., Cordeiro, J.G., Doostkam, S., Schulze-Bonhage, A., Stieglitz, T., and Rickert, J. (2011). First long term in vivo study on subdurally implanted Micro-ECoG electrodes, manufactured with a novel laser technology. Biomed. Microdevices *13*, 59–68. https://doi.org/10.1007/s10544-010-9471-9.

57. Degenhart, A.D., Eles, J., Dum, R., Mischel, J.L., Smalianchuk, I., Endler, B., Ashmore, R.C., Tyler-Kabara, E.C., Hatsopoulos, N.G., Wang, W., et al. (2016). Histological evaluation of a chronically-implanted electrocorticographic electrode grid in a non-human primate. J. Neural. Eng. *13*, 046019. https://doi.org/10.1088/1741-2560/13/4/046019.

58. Schendel, A.A., Nonte, M.W., Vokoun, C., Richner, T.J., Brodnick, S.K., Atry, F., Frye, S., Bostrom, P., Pashaie, R., Thongpang, S., et al. (2014). The effect of micro-ECoG substrate footprint on the meningeal tissue response. J. Neural. Eng. *11*, 046011. https://doi.org/10.1088/1741-2560/11/4/046011.

59. Schendel, A.A., Thongpang, S., Brodnick, S.K., Richner, T.J., Lindevig, B.D.B., Krugner-Higby, L., and Williams, J.C. (2013). A cranial window imaging method for monitoring vascular growth around chronically implanted micro-ECoG devices. J. Neurosci. Methods *218*, 121–130. https://doi.org/10.1016/J.JNEUMETH.2013.06.001.

60. Sauter-Starace, F., Ratel, D., Cretallaz, C., Foerster, M., Lambert, A., Gaude, C., Costecalde, T., Bonnet, S., Charvet, G., Aksenova, T., et al. (2019). Long-term sheep implantation of WIMAGINE®, a wireless 64-channel electrocorticogram recorder. Front. Neurosci. *13*, 847. https://doi.org/10.3389/fnins.2019.00847.

61. Arieli, A., Grinvald, A., and Slovin, H. (2002). Dural substitute for long-term imaging of cortical activity in behaving monkeys and its clinical implications. J. Neurosci. Methods *114*, 119–133. https://doi.org/10.1016/S0165-0270(01)00507-6.

62. Tybrandt, K., Khodagholy, D., Dielacher, B., Stauffer, F., Renz, A.F., Buzsáki, G., and Vörös, J. (2018). High-density stretchable electrode grids for chronic neural recording. Adv. Mater. *30*. 1706520. https://doi.org/10.1002/adma.201706520.

63. Ji, B., Guo, Z., Wang, M., Yang, B., Wang, X., Li, W., and Liu, J. (2018). Flexible polyimide-based hybrid opto- electric neural interface with 16 channels of micro-LEDs and electrodes. Microsyst. Nanoeng. *4*, 27. https://doi.org/10.1038/s41378-018-0027-0.

64. Luan, L., Robinson, J.T., Aazhang, B., Chi, T., Yang, K., Li, X., Rathore, H., Singer, A., Yellapantula, S., Fan, Y., et al. (2020). Recent advances in electrical neural interface engineering: minimal invasiveness, longevity, and scalability. Neuron *108*, 302–321. https://doi.org/10.1016/j.neuron.2020.10.011.

65. Yizhar, O., Fenno, L.E., Davidson, T.J., Mogri, M., and Deisseroth, K. (2011). Primer optogenetics in neural systems. Neuron *71*, 9–34. https://doi.org/10.1016/j.neuron.2011.06.004.

66. Deisseroth, K. (2015). Optogenetics: 10 years of microbial opsins in neuroscience. Nat. Neurosci. *18*, 1213–1225. https://doi.org/10.1038/nn.4091.

67. Han, X., Qian, X., Bernstein, J.G., Zhou, H.H., Franzesi, G.T., Stern, P., Bronson, R.T., Graybiel, A.M., Desimone, R., and Boyden, E.S. (2009). Millisecond-timescale optical control of neural dynamics in the nonhuman primate brain. Neuron *62*, 191–198. https://doi.org/10.1016/j.neuron.2009.03.011.

68. Diester, I., Kaufman, M.T., Mogri, M., Pashaie, R., Goo, W., Yizhar, O., Ramakrishnan, C., Deisseroth, K., and Shenoy, K.V. (2011). An optogenetic toolbox designed for primates. Nat. Neurosci. *14*, 387–397. https://doi.org/10.1038/nn.2749.

69. Cavanaugh, J., Monosov, I.E., McAlonan, K., Berman, R., Smith, M.K., Cao, V., Wang, K.H., Boyden, E.S., and Wurtz, R.H. (2012). Optogenetic inactivation modifies monkey visuomotor behavior. Neuron *76*, 901–907. https://doi.org/10.1016/j.neuron.2012.10.016.

70. Gerits, A., Farivar, R., Rosen, B.R., Wald, L.L., Boyden, E.S., and Vanduffel, W. (2012). Optogenetically induced behavioral and functional network changes in primates. Curr. Biol. *22*, 1722–1726. https://doi.org/10.1016/j.cub.2012.07.023.

71. Jazayeri, M., Lindbloom-Brown, Z., and Horwitz, G.D. (2012). Saccadic eye movements evoked by optogenetic activation of primate V1. Nat. Neurosci. *15*, 1368–1370. https://doi.org/10.1038/nn.3210.

72. Yazdan-Shahmorad, A., Silversmith, D.B., Kharazia, V., and Sabes, P.N. (2018). Targeted cortical reorganization using optogenetics in non-human primates. Elife *7*, e31034. https://doi.org/10.7554/eLife.31034.

73. Afraz, A., Boyden, E.S., and DiCarlo, J.J. (2015). Optogenetic and pharmacological suppression of spatial clusters of face neurons reveal their causal role in face gender discrimination. Proc. Natl. Acad. Sci. USA *112*, 6730–6735. https://doi.org/10.1073/pnas.1423328112.

74. Lu, Y., Truccolo, W., Wagner, F.B., Vargas-Irwin, C.E., Ozden, I., Zimmermann, J.B., May, T., Agha, N.S., Wang, J., and Nurmikko, A.V. (2015). Optogenetically induced spatiotemporal gamma oscillations and neuronal spiking activity in primate motor cortex. J. Neurophysiol. *113*, 3574–3587. https://doi.org/10.1152/jn.00792.2014.

75. Tremblay, S., Acker, L., Afraz, A., Albaugh, D.L., Amita, H., Andrei, A.R., Angelucci, A., Aschner, A., Balan, P.F., Basso, M.A., et al. (2020). An open resource for non-human primate optogenetics. Neuron *108*, 1075–1090.e6. https://doi.org/10.1016/j.neuron.2020.09.027.

76. Szerlip, N.J., Walbridge, S., Yang, L., Morrison, P.F., Degen, J.W., Jarrell, S.T., Kouri, J., Kerr, P.B., Kotin, R., Oldfield, E.H., and Lonser, R.R. (2007). Real-time imaging of convection-enhanced delivery of viruses and virus-sized particles. J. Neurosurg. *107*, 560–567. https://doi.org/10.3171/JNS-07/09/0560.

77. Khateeb, K., Griggs, D.J., Sabes, P.N., and Yazdan-Shahmorad, A. (2019). Convection enhanced delivery of optogenetic adeno-associated viral vector to the cortex of rhesus macaque under guidance of online MRI images. J. Vis. Exp.e59232 https://doi.org/10.3791/59232.

78. Griggs, D.J., Belloir, T., and Yazdan-Shahmorad, A. (2021). Large-scale neural interfaces for optogenetic actuators and sensors in non-human primates. In Integrated Sensors for Biological and Neural Sensing, H. Mohseni, ed. (SPIE), p. 17. https://doi.org/10.1117/12.2579431.

79. Ojemann, W.K., Griggs, D.J., Ip, Z., Caballero, O., Jahanian, H., Martinez-Conde, S., et al. (2020). A mri-based toolbox for neurosurgical planning in nonhuman primates. J. Vis. Exp. e61098. https://doi.org/10.3791/61098.

80. Macknik, S.L., Alexander, R.G., Caballero, O., Chanovas, J., Nielsen, K.J., Nishimura, N., Schaffer, C.B., Slovin, H., Babayoff, A., Barak, R., et al. (2019). Advanced circuit and cellular imaging methods in nonhuman primates. J. Neurosci. *39*, 8267–8274. https://doi.org/10.1523/JNEUROSCI.1168-19.2019.

81. Yazdan-Shahmorad, A., Tian, N., Kharazia, V., Samaranch, L., Kells, A., Bringas, J., He, J., Bankiewicz, K., and Sabes, P.N. (2018). Widespread optogenetic expression in macaque cortex obtained with MR-guided, convection enhanced delivery (CED) of AAV vector to the thalamus. J. Neurosci. Methods *293*, 347–358. https://doi.org/10.1016/j.jneumeth.2017.10.009.

82. Mehta, A.M., Sonabend, A.M., and Bruce, J.N. (2017). Convection-enhanced delivery. Neurotherapeutics *14*, 358–371. https://doi.org/10.1007/s13311-017-0520-4.

83. Aravanis, A.M., Wang, L.P., Zhang, F., Meltzer, L.A., Mogri, M.Z., Schneider, M.B., and Deisseroth, K. (2007). An optical neural interface: in vivo control of rodent motor cortex with integrated fiberoptic and optogenetic technology. J. Neural. Eng. *4*, S143–S156. https://doi.org/10.1088/1741-2560/4/3/S02.

84. Acker, L., Pino, E.N., Boyden, E.S., and Desimone, R. (2016). FEF inactivation with improved optogenetic methods. Proc. Natl. Acad. Sci. USA *113*, E7297–E7306. https://doi.org/10.1073/pnas.1610784113.

85. Tamura, K., Ohashi, Y., Tsubota, T., Takeuchi, D., Hirabayashi, T., Yaguchi, M., Matsuyama, M., Sekine, T., and Miyashita, Y. (2012). A glass-coated tungsten microelectrode enclosing optical fibers for optogenetic exploration in primate deep brain structures. J. Neurosci. Methods *211*, 49–57. https://doi.org/10.1016/J.JNEUMETH.2012.08.004.

86. Yazdan-Shahmorad, A., Diaz-Botia, C., Hanson, T., Ledochowitsch, P., Maharabiz, M.M., and Sabes, P.N. (2015). Demonstration of a setup for chronic optogenetic stimulation and recording across cortical areas in non-human primates. Proc.SPIE. p. 93052K. https://doi.org/10.1117/12.2080405.

87. Ohta, Y., Guinto, M.C., Tokuda, T., Kawahara, M., Haruta, M., Takehara, H., Tashiro, H., Sasagawa, K., Onoe, H., Yamaguchi, R., et al. (2021). Micro-LED array-based photo-stimulation devices for optogenetics in rat and macaque monkey brains. IEEE Access *9*, 127937–127949. https://doi.org/10.1109/ACCESS.2021.3111666.

88. Rajalingham, R., Sorenson, M., Azadi, R., Bohn, S., DiCarlo, J.J., and Afraz, A. (2021). Chronically implantable LED arrays for behavioral optogenetics in primates. Nat. Methods *18*, 1112–1116. https://doi.org/10.1038/s41592-021-01238-9.

89. Steude, A., Witts, E.C., Miles, G.B., and Gather, M.C. (2016). Arrays of microscopic organic LEDs for high-resolution optogenetics. Sci. Adv. *2*, e1600061. https://doi.org/10.1126/sciadv.1600061.

90. Mao, D., Li, N., Xiong, Z., Sun, Y., and Xu, G. (2019). Single-cell optogenetic control of calcium signaling with a high-density micro-LED array. iScience *21*, 403–412. https://doi.org/10.1016/j.isci.2019.10.024.

91. Owen, S.F., Liu, M.H., and Kreitzer, A.C. (2019). Thermal constraints on in vivo optogenetic manipulations. Nat. Neurosci. *22*, 1061–1065. https://doi.org/10.1038/S41593-019-0422-3.

92. Galvan, A., Stauffer, W.R., Acker, L., El-Shamayleh, Y., Inoue, K.I., Ohayon, S., and Schmid, M.C. (2017). Nonhuman primate optogenetics: recent advances and future directions. J. Neurosci. *37*, 10894–10903. https://doi.org/10.1523/JNEUROSCI.1839-17.2017.

93. Li, Y., Shi, Y., Song, J., Lu, C., Kim, T.i., Rogers, J.A., and Huang, Y. (2013). Thermal properties of microscale inorganic light-emitting diodes in a pulsed operation. J. Appl. Phys. *113*, 144505. https://doi.org/10.1063/1.4800858.

94. Kim, T.i., Jung, Y.H., Song, J., Kim, D., Li, Y., Kim, H.S., Song, I.S., Wierer, J.J., Pao, H.A., Huang, Y., et al. (2012). High-efficiency, microscale GaN light-emitting diodes and their thermal properties on unusual substrates. Small *8*, 1643–1649. https://doi.org/10.1002/smll.201200382.

95. Fang, S., Wang, W., Liang, J., Liang, Z., Qin, Y., and Lv, J. (2017). Heat dissipation analysis of bendable AlGaInP micro-LED arrays. AIP Adv. *7*, 015209. https://doi.org/10.1063/1.4975225.

96. Ji, B., Ge, C., Guo, Z., Wang, L., Wang, M., Xie, Z., Xu, Y., Li, H., Yang, B., Wang, X., et al. (2020). Flexible and stretchable opto-electric neural interface for low-noise electrocorticogram recordings and neuromodulation in vivo. Biosens. Bioelectron. *153*, 112009. https://doi.org/10.1016/j.bios.2020.112009.

97. Khan, W., Setien, M., Purcell, E., and Li, W. (2018). Micro-reflector integrated multichannel μLED optogenetic neurostimulator with enhanced intensity. Front. Mech. Eng. *4*, 1–10. https://doi.org/10.3389/fmech.2018.00017.

98. O'Doherty, J.E., Lebedev, M.A., Ifft, P.J., Zhuang, K.Z., Shokur, S., Bleuler, H., and Nicolelis, M.A.L. (2011). Active tactile exploration using a brain–machine–brain interface. Nature *479*, 228–231. https://doi.org/10.1038/nature10489.

99. Meador, K.J., Kapur, R., Loring, D.W., Kanner, A.M., and Morrell, M.J.; RNS® System Pivotal Trial Investigators (2015). Quality of life and mood in patients with medically intractable epilepsy treated with targeted responsive neurostimulation. Epilepsy Behav. *45*, 242–247. https://doi.org/10.1016/J.YEBEH.2015.01.012.

100. Pashaie, R., Anikeeva, P., Lee, J.H., Prakash, R., Yizhar, O., Prigge, M., Chander, D., Richner, T.J., and Williams, J. (2014). Optogenetic brain interfaces. IEEE Rev. Biomed. Eng. *7*, 3–30. https://doi.org/10.1109/RBME.2013.2294796.

101. Park, A.H., Lee, S.H., Lee, C., Kim, J., Lee, H.E., Paik, S.-B., Lee, K.J., and Kim, D. (2016). Optogenetic mapping of functional connectivity in freely moving mice via insertable wrapping electrode array beneath the skull. ACS Nano *10*, 2791–2802. https://doi.org/10.1021/acsnano.5b07889.

102. Brodnick, S.K., Ness, J.P., Richner, T.J., Thongpang, S., Novello, J., Hayat, M., Cheng, K.P., Krugner-Higby, L., Suminski, A.J., Ludwig, K.A., and Williams, J.C. (2019). μECoG recordings through a thinned skull. Front. Neurosci. *13*, 1017. https://doi.org/10.3389/FNINS.2019.01017/BIBTEX.

103. Park, J., Bong, J., Jung, Y.H., Kegel, J., Liu, B., Suminski, A.J., Brodnick, S.K., Jang, H., Yu, Z., Williams, J.C., and Ma, Z. (2021). Design and fabrication of blue LED-integrated graphene electrodes for neural stimulation and signal recording. ACS Appl. Electron. Mater. *3*, 4308–4316. https://doi.org/10.1021/acsaelm.1c00440.

104. Griggs, D.J., Bloch, J., Fisher, S., Ojemann, W.K.S., Coubrough, K.M., Chu, M., and Yazdan-shahmorad, A. (2022). Demonstration of an optimized large-scale optogenetic cortical interface for non-human primates. In 44th Annual International Conference of the IEEE Engineering in Medicine & Biology Society (EMBC), pp. 3081–3084.

105. Devon, J., Griggs, K.K., Stephen, A.P., Jia, W.C., William, K.S., and Ojemann, A.Y.-S. (2019). "Optimized large-scale optogenetic interface for non-human primates," Proc. SPIE 10866, Optogenetics and Optical Manipulation. 1086605. https://doi.org/10.1117/12.2511317.

106. Shtoyerman, E., Arieli, A., Slovin, H., Vanzetta, I., and Grinvald, A. (2000). Long-term optical imaging and spectroscopy reveal mechanisms underlying the intrinsic signal and stability of cortical maps in V1 of behaving monkeys. J. Neurosci. *20*, 8111–8121. https://doi.org/10.1523/JNEUROSCI.20-21-08111.2000.

107. Chen, L.M., Heider, B., Williams, G.V., Healy, F.L., Ramsden, B.M., and Roe, A.W. (2002). A chamber and artificial dura method for long-term optical imaging in the monkey. J. Neurosci. Methods *113*, 41–49. https://doi.org/10.1016/S0165-0270(01)00475-7.

108. Lu, H.D., Chen, G., Tanigawa, H., and Roe, A.W. (2010). A motion direction map in macaque V2. Neuron *68*, 1002–1013. https://doi.org/10.1016/J.NEURON.2010.11.020.

109. Slovin, H., Arieli, A., Hildesheim, R., and Grinvald, A. (2002). Long-term voltage-sensitive dye imaging reveals cortical dynamics in behaving monkeys. J. Neurophysiol. *88*, 3421–3438. https://doi.org/10.1152/jn.00194.2002.

110. Roe, A.W. (2007). Long-term optical imaging of intrinsic signals in anesthetized and awake monkeys. Appl. Opt. *46* (10), 1872–1880. https://doi.org/10.1364/AO.46.001872.

111. Nassi, J.J., Avery, M.C., Cetin, A.H., Roe, A.W., and Reynolds, J.H. (2015). Optogenetic activation of normalization in alert macaque visual cortex. Neuron *86*, 1504–1517. https://doi.org/10.1016/j.neuron.2015.05.040.

112. Seidemann, E., Chen, Y., Bai, Y., Chen, S.C., Mehta, P., Kajs, B.L., Geisler, W.S., and Zemelman, B.V. (2016). Calcium imaging with genetically encoded indicators in behaving primates. Elife *5*, e16178. https://doi.org/10.7554/ELIFE.16178.

113. Ruiz, O., Lustig, B.R., Nassi, J.J., Cetin, A., Reynolds, J.H., Albright, T.D., Callaway, E.M., Stoner, G.R., and Roe, A.W. (2013). Optogenetics through windows on the brain in the nonhuman primate. J. Neurophysiol. *110*, 1455–1467. https://doi.org/10.1152/jn.00153.2013.

114. Chen, L.M., Friedman, R.M., and Roe, A.W. (2005). Optical imaging of SI topography in anesthetized and awake squirrel monkeys. J. Neurosci. *25*, 7648–7659. https://doi.org/10.1523/JNEUROSCI.1990-05.2005.

115. Reynaud, A., Masson, G.S., and Chavane, F. (2012). Dynamics of local input normalization result from balanced short- and long-range intracortical interactions in area V1. J. Neurosci. *32*, 12558–12569. https://doi.org/10.1523/JNEUROSCI.1618-12.2012.

116. Michel, M.M., Chen, Y., Geisler, W.S., and Seidemann, E. (2013). An illusion predicted by V1 population activity implicates cortical topography in shape perception. Nat. Neurosci. *16*, 1477–1483. https://doi.org/10.1038/nn.3517.

117. Omer, D.B., Fekete, T., Ulchin, Y., Hildesheim, R., and Grinvald, A. (2019). Dynamic patterns of spontaneous ongoing activity in the visual cortex of anesthetized and awake monkeys are different. Cereb. Cortex *29*, 1291–1304. https://doi.org/10.1093/cercor/bhy099.

118. Cao, G., Platisa, J., Pieribone, V.A., Raccuglia, D., Kunst, M., and Nitabach, M.N. (2013). Genetically targeted optical electrophysiology in intact neural circuits. Cell *154*, 904–913. https://doi.org/10.1016/J.CELL.2013.07.027.

119. Knöpfel, T., Gallero-Salas, Y., and Song, C. (2015). Genetically encoded voltage indicators for large scale cortical imaging come of age. Curr. Opin. Chem. Biol. *27*, 75–83. https://doi.org/10.1016/J.CBPA.2015.06.006.

120. Vogt, N. (2014). Sensors and probes: visualizing voltage. Nat. Methods *11*, 710–711. https://doi.org/10.1038/nmeth.3018.

121. Beck, C., and Gong, Y. (2019). A high-speed, bright, red fluorescent voltage sensor to detect neural activity. Sci. Rep. *9*, 15878. https://doi.org/10.1038/s41598-019-52370-8.

122. Adam, Y., Kim, J.J., Lou, S., Zhao, Y., Xie, M.E., Brinks, D., Wu, H., Mostajo-Radji, M.A., Kheifets, S., Parot, V., et al. (2019). Voltage imaging and optogenetics reveal behavior dependent changes in hippocampal dynamics. Nature *569*, 413–417. https://doi.org/10.1038/S41586-019-1166-7.

123. Nauhaus, I., Nielsen, K.J., Disney, A.A., and Callaway, E.M. (2012). Orthogonal micro-organization of orientation and spatial frequency in primate primary visual cortex. Nat. Neurosci. *15*, 1683–1690. https://doi.org/10.1038/NN.3255.

124. Chatterjee, S., Ohki, K., and Reid, R.C. (2021). Chromatic micromaps in primary visual cortex. Nat. Commun. *12*, 2315. https://doi.org/10.1038/s41467-021-22488-3.

125. Heider, B., Nathanson, J.L., Isacoff, E.Y., Callaway, E.M., and Siegel, R.M. (2010). Two-photon imaging of calcium in virally transfected striate cortical neurons of behaving monkey. PLoS One *5*, e13829. https://doi.org/10.1371/JOURNAL.PONE.0013829.

126. Sadakane, O., Masamizu, Y., Watakabe, A., Terada, S.I., Ohtsuka, M., Takaji, M., Mizukami, H., Ozawa, K., Kawasaki, H.,

Matsuzaki, M., et al. (2015). Long-term two-photon calcium imaging of neuronal populations with subcellular resolution in adult non-human primates. Cell Rep. *13*, 1989–1999. https://doi.org/10.1016/J.CELREP.2015.10.050.

127. Yamada, Y., Matsumoto, Y., Okahara, N., and Mikoshiba, K. (2016). Chronic multiscale imaging of neuronal activity in the awake common marmoset. Sci. Rep. *6*, 35722. https://doi.org/10.1038/srep35722.

128. Li, M., Liu, F., Jiang, H., Lee, T.S., and Tang, S. (2017). Long-term two-photon imaging in awake macaque monkey. Neuron *93*, 1049–1057.e3. https://doi.org/10.1016/J.NEURON.2017.01.027.

129. Ebina, T., Masamizu, Y., Tanaka, Y.R., Watakabe, A., Hirakawa, R., Hirayama, Y., Hira, R., Terada, S.I., Koketsu, D., Hikosaka, K., et al. (2018). Two-photon imaging of neuronal activity in motor cortex of marmosets during upper-limb movement tasks. Nat. Commun. *9*, 1879. https://doi.org/10.1038/s41467-018-04286-6.

130. Trautmann, E.M., O'Shea, D.J., Sun, X., Marshel, J.H., Crow, A., Hsueh, B., Vesuna, S., Cofer, L., Bohner, G., Allen, W., et al. (2021). Dendritic calcium signals in rhesus macaque motor cortex drive an optical brain-computer interface. Nat. Commun. *12*, 3689. https://doi.org/10.1038/s41467-021-23884-5.

131. Zeng, H.H., Huang, J.F., Chen, M., Wen, Y.Q., Shen, Z.M., and Poo, M.M. (2019). Local homogeneity of tonotopic organization in the primary auditory cortex of marmosets. Proc. Natl. Acad. Sci. USA *116*, 3239–3244. https://doi.org/10.1073/pnas.1816653116.

132. Kim, C.K., Adhikari, A., and Deisseroth, K. (2017). Integration of optogenetics with complementary methodologies in systems neuroscience. Nat. Rev. Neurosci. *18*, 222–235. https://doi.org/10.1038/NRN.2017.15.

133. Rickgauer, J.P., Deisseroth, K., and Tank, D.W. (2014). Simultaneous cellular-resolution optical perturbation and imaging of place cell firing fields. Nat. Neurosci. *17*, 1816–1824. https://doi.org/10.1038/nn.3866.

134. Marshel, J.H., Kim, Y.S., Machado, T.A., Quirin, S., Benson, B., Kadmon, J., Raja, C., Chibukhchyan, A., Ramakrishnan, C., Inoue, M., et al. (2019). Cortical layer–specific critical dynamics triggering perception. Science *365*, eaaw5202. https://doi.org/10.1126/SCIENCE.AAW5202.

135. Jennings, J.H., Kim, C.K., Marshel, J.H., Raffiee, M., Ye, L., Quirin, S., Pak, S., Ramakrishnan, C., and Deisseroth, K. (2019). Interacting neural ensembles in orbitofrontal cortex for social and feeding behaviour. Nature *565*, 645–649. https://doi.org/10.1038/s41586-018-0866-8.

136. Inoue, K., Karasuyama, M., Nakamura, R., Konno, M., Yamada, D., Mannen, K., Nagata, T., Inatsu, Y., Yawo, H., Yura, K., et al. (2021). Exploration of natural red-shifted rhodopsins using a machine learning-based Bayesian experimental design. Commun. Biol. *4*, 362. https://doi.org/10.1038/s42003-021-01878-9.

137. Sengupta, A., Chaffiol, A., Macé, E., Caplette, R., Desrosiers, M., Lampič, M., Forster, V., Marre, O., Lin, J.Y., Sahel, J.-A., et al. (2016). Red-shifted channelrhodopsin stimulation restores light responses in blind mice, macaque retina, and human retina. EMBO Mol. Med. *8*, 1248–1264. https://doi.org/10.15252/EMMM.201505699.

138. Ju, N., Jiang, R., Macknik, S.L., Martinez-Conde, S., and Tang, S. (2018). Long-term all-optical interrogation of cortical neurons in awake-behaving nonhuman primates. PLoS Biol. *16*, e2005839. https://doi.org/10.1371/journal.pbio.2005839.

139. O'Shea, D.J., Trautmann, E., Chandrasekaran, C., Stavisky, S., Kao, J.C., Sahani, M., Ryu, S., Deisseroth, K., and Shenoy, K.V. (2017). The need for calcium imaging in nonhuman primates: new motor neuroscience and brain-machine interfaces. Exp. Neurol. *287*, 437–451. https://doi.org/10.1016/j.expneurol.2016.08.003.

140. Choi, W.J. (2019). Optical coherence tomography angiography in preclinical neuroimaging. Biomed. Eng. Lett. *9*, 311–325. https://doi.org/10.1007/S13534-019-00118-8.

141. Khateeb, K., Yao, Z., Kharazia, V.N., Burunova, E.P., Song, S., Wang, R., and Yazdan-Shahmorad, A. (2019). A practical method for creating targeted focal ischemic stroke in the cortex of nonhuman primates. Annu. Int. Conf. IEEE Eng. Med. Biol. Soc. *2019*, 3515–3518. https://doi.org/10.1109/EMBC.2019.8857741.

142. Khateeb, K., Bloch, J., Zhou, J., Rahimi, M., Griggs, D.J., Kharazia, V.N., Le, M.N., Wang, R.K., and Yazdan-Shahmorad, A. (2022). A versatile toolbox for studying cortical physiology in primates. Cell Rep. Methods *2*, 100183. https://doi.org/10.1016/J.CRMETH.2022.100183.

143. Yao, Z., and Yazdan-Shahmorad, A. (2018). A quantitative model for estimating the scale of photochemically induced ischemic stroke. Annu. Int. Conf. IEEE Eng. Med. Biol. Soc. *2018*, 2744–2747. https://doi.org/10.1109/EMBC.2018.8512880.

144. Zhou, J., Khateeb, K., Gala, A., Rahimi, M., Griggs, D.J., Ip, Z., and Yazdan-Shahmorad, A. (2022). Neuroprotective effects of electrical stimulation following ischemic stroke in non-human primates. Annu. Int. Conf. IEEE Eng. Med. Biol. Soc. *2022*, 3085–3088. https://doi.org/10.1109/EMBC48229.2022.9871335.

145. Mcandrew, R., and Helms Tillery, S.I. (2016). Laboratory primates: their lives in and after research. Temperature *3*, 502–508. https://doi.org/10.1080/23328940.2016.1229161.

146. Russell, W.M.S., and Burch, R.L. (1959). The Principles of Humane Experimental Technique (Methuen).

147. Blakemore, C., MaCarthur Clark, J., Nevalainen, T., Oberdorfer, M., and Sussman, A. (2012). Implementing the 3Rs in neuroscience research: a reasoned approach. Neuron *75*, 948–950. https://doi.org/10.1016/J.NEURON.2012.09.001.

148. Strech, D., and Dirnagl, U. (2019). 3Rs missing: animal research without scientific value is unethical. BMJ Open Sci. *3*. bmjos-2018-000048. https://doi.org/10.1136/BMJOS-2018-000048.

149. Rübel, O., Tritt, A., Ly, R., Dichter, B.K., Ghosh, S., Niu, L., Soltesz, I., Svoboda, K., Frank, L., and Bouchard, K.E. (2022). The Neurodata without Borders ecosystem for neurophysiological data science. Prepirnt at. bioRxiv. https://doi.org/10.1101/2021.03.13.435173.

150. Markiewicz, C.J., Gorgolewski, K.J., Feingold, F., Blair, R., Halchenko, Y.O., Miller, E., Hardcastle, N., Wexler, J., Esteban, O., Goncavles, M., et al. (2021). The openneuro resource for sharing of neuroscience data. Elife *10*, e71774. https://doi.org/10.7554/ELIFE.71774.

151. Milham, M.P., Ai, L., Koo, B., Xu, T., Amiez, C., Balezeau, F., Baxter, M.G., Blezer, E.L.A., Brochier, T., Chen, A., et al. (2018). An open resource for non-human primate imaging. Neuron *100*, 61–74.e2. https://doi.org/10.1016/J.NEURON.2018.08.039.

152. Basso, M.A., Frey, S., Guerriero, K.A., Jarraya, B., Kastner, S., Koyano, K.W., Leopold, D.A., Murphy, K., Poirier, C., Pope, W., et al. (2021). Using non-invasive neuroimaging to enhance the care, well-being and experimental outcomes of laboratory non-human primates (monkeys). Neuroimage *228*, 117667. https://doi.org/10.1016/J.NEUROIMAGE.2020.117667.

153. Johnson, L.S.M. (2020). In The Trouble with Animal Models in Brain Research BT - Neuroethics and Nonhuman Animals, L.S.M. Johnson, A. Fenton, and A. Shriver, eds. (Springer International Publishing), pp. 271–286. https://doi.org/10.1007/978-3-030-31011-0_16.

154. Kellmeyer, P. (2018). Big brain data: on the responsible use of brain data from clinical and consumer-directed neurotechnological devices. Neuroethics *14*, 83–98. https://doi.org/10.1007/S12152-018-9371-X.

155. Yuste, R., Goering, S., Arcas, B.A.Y., Bi, G., Carmena, J.M., Carter, A., Fins, J.J., Friesen, P., Gallant, J., Huggins, J.E., et al. (2017). Four ethical priorities for neurotechnologies and AI. Nature *551*, 159–163. https://doi.org/10.1038/551159a.

156. Schönau, A., Dasgupta, I., Brown, T., Versalovic, E., Klein, E., Goering, S., and Sch€, A. (2021). Mapping the dimensions of agency. AJOB Neurosci. *12*, 172–186. https://doi.org/10.1080/21507740.2021.1896599.